NASA MEMO 3-3-59L

NASA

MEMORANDUM

WIND-TUNNEL INVESTIGATION OF THE EFFECT OF ANGLE OF ATTACK AND FLAPPING-HINGE OFFSET ON PERIODIC BENDING MOMENTS AND FLAPPING OF A SMALL ROTOR

By John Locke McCarty, George W. Brooks, and Domenic J. Maglieri

Langley Research Center
Langley Field, Va.

NATIONAL AERONAUTICS AND SPACE ADMINISTRATION

WASHINGTON

March 1959

NATIONAL AERONAUTICS AND SPACE ADMINISTRATION

MEMORANDUM 3-3-59L

WIND-TUNNEL INVESTIGATION OF THE EFFECT OF ANGLE OF ATTACK AND FLAPPING-HINGE OFFSET ON PERIODIC BENDING MOMENTS AND FLAPPING OF A SMALL ROTOR

By John Locke McCarty, George W. Brooks,
and Domenic J. Maglieri

SUMMARY

A two-blade rotor having a diameter of 4 feet and a solidity of 0.037 was tested in the Langley 300-MPH 7- by 10-foot tunnel to obtain information on the effect of certain rotor variables on the blade periodic bending moments and flapping angles during the various stages of transformation between the helicopter and autogiro configuration. Variables studied included collective pitch angle, flapping-hinge offset, rotor angle of attack, and tip-speed ratio.

The results show that the blade periodic bending moments generally increase with tip-speed ratio up into the transition region, diminish over a certain range of tip-speed ratio, and increase again at higher tip-speed ratios. Above the transition region, the bending moments increase with collective pitch angle and rotor angle of attack. The absence of a flapping hinge results in a significant amplification of the periodic bending moments, the magnitudes of which increase with tip-speed ratio. When the flapping hinge is used, an increase in flapping-hinge offset results in reduced period bending moments.

The aforementioned trends exhibited by the bending moments for changes in the variables are essentially duplicated by the periodic flapping motions. The existence of substantial amounts of blade stall increased both the periodic bending moments and the flapping angles.

Harmonic analysis of the bending moments shows significant contributions of the higher harmonics, particularly in the transition region.

INTRODUCTION

In the quest for a machine possessing both hovering and high-speed capabilities, there is a continuous need for information on the dynamic behavior of rotor systems.

Prior to World War II, much work was done on the analytical and experimental determination of the characteristics of rotors, including the determination of flapping angles, lift-drag ratios, and so forth. (See, e.g., refs. 1 to 5.) Although many of the results of these studies are applicable to helicopters (which operate primarily at negative rotor angles of attack), the emphasis was on autogiros (which operate at positive rotor angles of attack). The lack of engines of suitable power-weight ratio to permit hovering flight was probably the significant factor in the early emphasis of the autogiro.

During and following World War II, the helicopter became a reality and has developed rapidly. The forward velocity of the pure helicopter configuration, however, is limited because of blade stall on the retreating blades and compressibility effects on the advancing blades. A possible way of achieving higher speed in forward flight while preserving the salient advantages of the helicopter for hovering and vertical flight is to unload the rotor in forward flight by providing the vehicle with a conventional lift surface and an airplane type of propulsion system (refs. 6 to 8). This convertiplane-type configuration places the rotor again in a semiautogiro configuration.

Although much information exists on the steady aerodynamics and blade flapping angles of the autorotating rotor (refs. 1 to 5) and on the periodic flapping angles and bending moments of helicopter rotors (refs. 5 and 9 to 11), very little has been published on the variation of periodic rotor-blade bending moments or flapping angles in the various stages of transformation between the helicopter and autogiro configurations. In an effort to obtain information on blade periodic bending moments and flapping angles in these flight regions, a dynamic model of a two-blade rotor was tested in the Langley 300-MPH 7- by 10-foot tunnel over a range of tip-speed ratios from 0 to 0.30 and at positive rotor angles of attack from 0° to 60°. Other parameters studied were collective pitch angle and blade flapping-hinge offset. The results of this study are reported herein.

SYMBOLS

EI	blade flapwise bending stiffness, lb-in.^{2}
e	distance from flapping hinge to axis of rotation, ft unless otherwise stated

M double amplitude of blade periodic flapwise bending moments, in-lb

R blade radius, ft unless otherwise stated

r radial distance to blade element, ft unless otherwise stated

V tunnel velocity, fps

v induced velocity at rotor (always positive), fps

α rotor angle of attack (angle between flight path and plane perpendicular to axis of no feathering, in this case, the shaft axis) positive when axis is inclined rearward, deg

$\bar{\beta}$ double amplitude of blade periodic flapping angle, deg

θ blade collective pitch angle, deg

λ rotor inflow ratio, $\frac{V \sin \alpha - v}{R\Omega}$

μ tip-speed ratio, $\frac{V \cos \alpha}{R\Omega}$

ψ blade azimuth angle, deg

Ω rotor angular velocity, radians/sec

Subscripts:

1 blade station at $r/R = 0.25$

2 blade station at $r/R = 0.42$

3 blade station at $r/R = 0.625$

4 blade station at $r/R = 0.833$

r reference bending moment

APPARATUS AND TEST PROCEDURE

Apparatus

The test apparatus includes the rotor and rotor drive system, the model support, and the wind tunnel. Pertinent details of the apparatus are given as follows:

Rotor characteristics and configurations.- The rotor configurations studied in this investigation include a two-blade fixed-at-root rotor and a two-blade flapping rotor having offsets of 0, 5, and 10 percent of the rotor radius. All tests were conducted with the same blades; only the root fittings were changed to obtain the desired configuration. In each case, the rotor had a diameter of 4 feet and a solidity of 0.037. The blades were rectangular in plan form with a chord of 1.4 inches, untwisted, and had an NACA 0012 airfoil section. The blades were scaled in stiffness and weight to be representative of the dynamic characteristics of present-day helicopter blades. This scaling was accomplished by forming the blade profile of cellulose-acetate material to an aluminum spar having the proper weight and stiffness distributions.

The blades were attached to the rotor shaft by means of root fittings as shown by figures 1 and 2. Figure 1 shows the construction of the fixed-at-root condition.

The particular flapping configuration shown in figure 2 corresponds to the 5-percent-offset condition; however, the other offset fittings were constructed in the same manner by varying the lengths of the hub and the extension plates. Drag hinges were used in all tests, and in all cases were located at $\frac{r}{R} = 0.15$. Drag-hinge dampers were used on the flapping configurations only. As indicated in the figure, blade-retention straps were provided to transmit the centrifugal forces to the hub. A change in blade offset was accomplished by removing the drag-hinge pin and changing the offset fitting. Figure 2 shows that the blade collective pitch angle was unaffected by changes in offset fittings since the provisions to change the pitch angle were outboard of the drag-hinge pin.

The stiffness and weight distributions along the span of one blade for the various root fittings are given in figures 3 and 4, respectively. Frequency diagrams for the blade with the four root fittings are presented in figure 5 in which the uncoupled natural frequencies of the first three bending modes and the harmonics of the rotor frequency are plotted as functions of the rotor speed. The natural frequencies of the nonrotating blade were measured experimentally, and the natural frequencies of the rotating blade were determined by using the procedure of reference 12.

Model support and rotor drive system:- The model was supported from the ceiling of the tunnel test section by means of a rigid cantilever beam, hereinafter designated as the model support, which positioned the rotor approximately on the center line of the test section at the center of the tunnel balance system. The model and the model support are shown in figure 6, and a sketch of the support with appropriate dimensions is given in figure 7. Figure 7 also shows the method used in changing the

rotor angle of attack. Changes in rotor angle of attack were accomplished by varying the length of the angle-of-attack control arm.

The rotor system, which included both the slipring assembly and the rotor shaft, was driven by a commercial utility type of electric drill motor. The rotor speed was controlled by varying the voltage to this drill motor.

Wind-tunnel characteristics.- The model was tested in the Langley 300-MPH 7- by 10-foot tunnel and was mounted in the tunnel test section as shown in figure 6. Nominal dimensions of the test section are 7 feet high, 10 feet wide, and 15 feet long. The position of the model in the tunnel corresponded to the position for best flow conditions as indicated by flow surveys.

No wind-tunnel corrections are applied to the data presented in this paper because of the lack of information applicable to the corrections of the periodic phenomena studied. However, it is reasonable to expect some effect of wind-tunnel interference on the data because of blockage, flow angularity, velocity variations, and so forth, particularly at the lower tunnel velocities and at high disk loadings.

Instrumentation

One blade of the rotor was instrumented to measure the blade flapping angle and blade flapwise bending moments. The blade flapping angle was measured by means of the electrical-resistance-wire flapping indicator shown in figure 2. The blade bending moments were measured at four spanwise stations (r/R = 0.25, 0.42, 0.625, and 0.833) by means of strain-gage bridges mounted on the spar. The periodic variation of rotor thrust was obtained from a strain-gage bridge mounted on the rotor balance which is indicated in figure 7. Bridges were also mounted on the rotor balance to indicate hub moments but these were not used during this investigation.

A rotor-speed timer was used to record the rotor speed which was set during the tests by controlling the motor voltage and checked by means of stroboscopic lighting.

The velocity of the air in the tunnel was measured by means of a calibrated commercial air meter and checked by means of a calibrated sphere. Both of these were mounted on a common stand which is located about 1 rotor diameter upstream of the rotor, approximately at the height of the rotor, and about 2 feet to one side of the tunnel axis as shown in the lower right-hand corner of figure 6.

A slipring-brush assembly, mounted on the rotor shaft within the housing which is shown in figure 7, was used to transmit the signals from the rotor to the control station where they were recorded, together with the wind velocity, on oscillograph records. Sample oscillograph records are shown in figure 8 and discussed in subsequent sections.

Test Procedure

The model was tested over a range of wind-tunnel velocities at rotor angles of attack from 0° to 60° in increments of 10°. For each rotor angle of attack there existed a maximum tunnel velocity (imposed by structural limitations of the model) at which the tests could be conducted. This limitation is such that the maximum tunnel velocity decreases as the rotor angle of attack increases.

The testing technique involved increasing the rotor speed of the model to the test value of 800 rpm at which point the tunnel was brought up to the maximum desired speed for that test condition. After the flow in the tunnel had become well established at that speed, the tunnel power was shut off. As the tunnel speed decreased, oscillograph records of the strain-gage responses were taken and the corresponding tunnel velocity was recorded. The rate of decay of forward speed was low enough to permit records to be taken at velocity intervals of 2 fps or less.

Each of the four root fittings was tested at collective pitch angles of 0°, 3°, and 6°. In order to minimize the errors associated with frequent changes of blade collective pitch angle, all tests for one pitch-angle setting were made before repeating the test procedure for a different pitch-angle setting.

METHOD OF ANALYSIS AND PRESENTATION

The procedure followed in the analysis of the data to obtain the periodic blade bending moments and periodic blade flapping angles may be described as follows. The double amplitudes of the envelope of the strain-gage trace deflections and the flapping-angle trace deflections of the blade were measured from the oscillograph records taken during the wind-tunnel tests. These trace deflections were then interpreted by means of calibration curves to obtain the bending moments and flapping angles of the blade. Calibration of the blade consisted of static tests which involved applying known weights to the blade tip for the bending moments and deflecting the blade through a range of known angles for flapping. The use of a single spar to transmit blade loads permitted a

simple calibration technique inasmuch as coupling of bending and torsion deformations could be avoided. The measured bending moments and flapping angles were then plotted as a function of tunnel speed. Figures 9 and 10 are typical of these plots and show, respectively, the double amplitude of the blade periodic bending moments at a selected radial location and the periodic flapping angles for one configuration over the range of test conditions.

Because of the large amount of data obtained, it was decided to assemble the data in tables and to present representative samples of these data in figures as required for discussion of the significant points or trends found during the investigation. Tables I to IV, which contain these data, were obtained by first fairing curves through the data points as shown in figures 9 and 10. The faired curves were then read for specific values of tip-speed ratio μ and tabulated for the appropriate configuration and rotor angle of attack. The tables show the double-amplitude blade periodic flapping angle β and the double-amplitude blade periodic bending moments at the four radial strain-gage locations M_1 to M_4. The representative samples of these data are plotted as a function of appropriate independent variables to point out the significant results of the study.

RESULTS AND DISCUSSION

Bending Moments

The measured, double-amplitude, periodic bending moments of the blade are presented in tables I to IV. The tables contain the data obtained at the four spanwise blade stations (r/R = 0.25, 0.42, 0.625, and 0.833) for all test conditions. Representative samples of data are selected from the tables and plotted in figures 11 to 20 to aid in the discussion of the results and trends observed.

Inasmuch as blade stall is a significant factor with respect to periodic bending moments and flapping angles of the blade, it was believed that an indication of the proximity of stall would be useful. Consequently, short vertical lines are shown on the curves of appropriate figures to indicate the value of μ at which the stall angle of attack of the blade element (at $\psi = 270^\circ$) occurs when the tangential velocity is equal to $0.4\Omega R$. This criterion (ref. 13) for rotors operating at positive angles of attack appears to give a good indication of the tip-speed ratio at which the effects of stall become significant. For the Reynolds number of these blades (approximately 63,000), the data of reference 14 indicated the blade-element angle at stall to be 8°, which was used to establish the stall limits.

In the presentation of the data in figures 11 to 16, the data are plotted to show, first, the variation of bending moment at the inboard station ($r/R = 0.25$) with tip-speed ratio for different values of collective pitch angle, rotor angle of attack, and flapping-hinge offset (figs. 11, 13, and 15), and second, the variation of bending moment with r/R for six different values of tip-speed ratio (figs. 12, 14, and 16). Figures 17 to 20 present the results of a harmonic analysis of the records from which the samples shown in figure 8 were obtained. A discussion of the results presented in these figures follows.

Effect of blade collective pitch angle.- Figures 11 and 12 present representative samples of data chosen to demonstrate the effect of blade collective pitch angle on the double amplitude of the blade periodic bending moments. Figure 11, which presents the data for $e/R = 0$, $\alpha = 20^\circ$, and $r/R = 0.25$, shows bending moment plotted as a function of tip-speed ratio for the three values of blade collective pitch angle tested. The figure shows that, at a given value of tip-speed ratio, the bending moment generally increases with collective pitch angle; this increase is rather consistent and of a significant order of magnitude throughout the range of tip-speed ratios. The curves also show, for collective pitch angles of 3° and 6°, the characteristic variation of bending moment with tip-speed ratio, which will be further discussed in subsequent sections, is manifest in a maximum in the region of transition followed by a minimum at a value of μ of 0.12. This fluctuation of bending moment with tip-speed ratio is such that the bending moment for $\theta = 3^\circ$ at $\mu = 0.05$ is greater than the bending moment for $\theta = 6^\circ$ at $\mu = 0.12$.

Figure 12, which presents data for $e/R = 0$ and $\alpha = 20^\circ$, shows the distribution of double-amplitude bending moments along the span (as indicated by the four strain-gage stations) for six specific values of tip-speed ratio. The effect of collective pitch angle may be observed by comparing the relative magnitudes of the curves for the respective collective pitch-angle settings for the given tip-speed ratios. This figure shows that the magnitude of the bending moment generally increases with an increase in collective pitch angle at all spanwise stations.

In figure 12, and in subsequent figures which show the bending moment as a function of a fraction of blade radius, it is observed that the bending moment at $r/R = 0.42$ is consistently less than corresponding moments at $r/R = 0.25$ and at $r/R = 0.625$. This distribution is apparently due to the fact that a significant portion of the blade moments involves bending in the second elastic mode which, because of the characteristic of the curvature of this mode, exhibits very little moment in the vicinity of $r/R = 0.42$. (See fig. 3 of ref. 9.)

Effect of rotor angle of attack.- The effect of rotor angle of attack on the periodic bending moments is conveniently shown by the

samples of data presented in figures 13 and 14. Figure 13 presents the double-amplitude bending moment as a function of tip-speed ratio for a representative case ($e/R = 0$, $r/R = 0.25$, and $\theta = 3^\circ$) for the complete range of rotor angle of attack. The data presented in this figure show several typical trends. First, the bending moments measured for $\alpha = 0^\circ$ are not consistent with the results obtained at small positive angles of attack, say at $\alpha = 10^\circ$. Second, there are definite maximums in the bending moments in the so-called transition range (used in this paper to designate the intermediate range of μ of approximately 0.02 to 0.12) for the lower values of rotor angle of attack ($\alpha = 0^\circ$, 10°, and 20°) which is reminiscent of the increase in bending moments found for blades operated in the negative rotor-angle-of-attack or helicopter regime (refs. 9 to 11). Following this peak, the bending moments subside and increase again at the higher values of μ. Third, with the exception of the case for $\alpha = 0^\circ$, the bending moments at the values of μ beyond transition range generally increase with rotor angle of attack. Whether the bending moment increases or decreases with a corresponding increase or decrease in rotor angle of attack is contingent upon the magnitude of the tip-speed ratio. Furthermore, this figure shows that, as the tip-speed ratio is increased from $\mu = 0.045$ to $\mu = 0.15$, the angle of attack which yields the highest bending moment varies from $\alpha = 20^\circ$ to $\alpha = 40^\circ$. This variation is perhaps better shown in figure 14 in which the double-amplitude bending moment is plotted against fraction of blade radius for the four spanwise strain-gage locations at rotor angles of attack of 0°, 20°, and 40° for six specific values of tip-speed ratio. Figure 14 also shows that the spanwise distribution of the double-amplitude bending moment essentially remains unchanged as the rotor angle of attack and tip-speed ratio are varied.

Effect of flapping hinge and magnitude of flapping-hinge offset.- The effect of the flapping hinge and the magnitude of flapping-hinge offset on the double-amplitude bending moments of the blade is illustrated by the representative samples of data ($\alpha = 20^\circ$ and $\theta = 3^\circ$) presented in figures 15 and 16. Figure 15 presents the bending moments measured at the inboard strain-gage location ($r/R = 0.25$) for the fixed-at-root configuration as well as for the three flapping configurations. These data show that the bending moments are substantially higher for the fixed-at-root configuration than for the flapping configurations as might be expected. The figure also shows the typical maximums in bending moments at low tip-speed ratios, but except for the very low tip-speed ratios, a beneficial effect of offset (i.e., a reduction in bending moment) is evident. It is also quite evident from figure 15 that the beneficial effect of the flapping rotor as compared with the cantilever rotor is more pronounced at the higher values of μ. This latter effect is again emphasized in figure 16 in which the bending moments are presented as a function of r/R for discrete values of μ. This figure shows that the use of a flapping hinge substantially

reduced the moments over the inboard portion of the blade as expected but that the moments on the outboard half of the blades are essentially unchanged. A reduction in the double-amplitude bending moments with increasing flapping-hinge offset is also indicated for the configurations tested herein. In general, the effects of flapping-hinge offset on the bending moments would be expected to be dependent upon the mass distribution over the inboard portion of the blade.

Effect of tip-speed ratio.- The effect of tip-speed ratio on blade bending moments is evident in figures 11 to 16. These data show that, in general, the characteristic variation of bending moment with tip-speed ratio at positive rotor angles of attack, which simulates the unloaded rotor or autogiro state, is similar to that observed for the rotor operated at negative angles of attack which is the fundamental working condition for the helicopter. This characteristic variation in bending moment is typified by a maximum in the bending-moment curve at some tip-speed ratio in the transition range, followed by a reduction in bending moment until a minimum is reached. As the tip-speed ratio is increased beyond the value at which the minimum occurs, there appears to be a rather consistent and substantial increase in blade bending moment. The existence of the maximum in the bending moments during the transition range is associated with high asymmetries of the induced flow occurring in this region. The data for the range of variables covered in this investigation indicate that the tip-speed ratios corresponding to the maximum and minimum, respectively, increase somewhat with blade collective pitch angle (fig. 11) and decrease with rotor angle of attack (fig. 13). These results demonstrate a tendency for the maximum and minimum to occur at a constant value of the rotor-disk lift coefficient.

An inspection of the samples of oscillograph records presented in figure 8 suggests that there is a substantial change in the harmonic content of the double-amplitude bending moments as the tip-speed ratio is varied. In order to obtain a qualitative idea of the magnitude of the changes in harmonic content, the records from which the samples of figure 8 were taken were harmonically analyzed and the results are presented in figures 17 to 20 for the spanwise locations of $r/R = 0.25$, 0.42, 0.625, and 0.833, respectively. The harmonic analysis was performed by averaging the ordinates at each of 24 points per cycle for five cycles prior to the computation of the harmonic components.

As a preliminary to further discussion of the harmonic analysis, it is helpful to refer to the frequency diagram of the blades which is presented in figure 5. The case being considered is that of $e/R = 0$ and the corresponding natural frequencies are shown by the long-dashed lines. At the operating rotor speed (indicated by the vertical line on the figure at 13.3 cps), the ratios of the natural frequencies of

the first three elastic bending modes to the rotor speed are approximately 2.5, 4.6, and 7.9, respectively. From a resonance standpoint, amplification of the bending moments would be expected due to the second, third, fourth, fifth, and, particularly, the eighth harmonic components of the aerodynamic loading, if such components exist. Previous experience (refs. 6, 9, and 10) with helicopter rotors indicates that all harmonic components of aerodynamic loading do exist at least to some degree, with the magnitude of the lower harmonics predominating particularly for tip-speed ratios corresponding to the transition and high-speed-flight regimes. Thus, it is expected that some evidence of resonance amplification will exist in the harmonic analysis of the bending moments.

In each of figures 17 to 20, the harmonic component which has the maximum amplitude is used as a reference, and the bending moment associated with it is given in the legend. The figures show, in general, that the expected resonance amplifications do exist.

An interesting variation of the harmonic content as a function of blade radius is afforded by comparison of the figures for the different values of r/R for $\alpha = 0^\circ$ or $\alpha = 20^\circ$. For example, in the case of $\alpha = 0^\circ$, at $r/R = 0.25$ (fig. 17(a)) the second harmonic component has the largest amplitude; whereas, for $r/R = 0.625$ (fig. 19(a)) the first harmonic component is the largest.

At the high values of μ, the figures show that at $\alpha = 0^\circ$, the harmonics are rather uniformly distributed as compared with those at $\alpha = 20^\circ$ where the lower order harmonics predominate.

Flapping Angles

Experimental results.- The flapping-angle data are presented in tables I to IV. A study of the data shows that the results are in general agreement with information presented for larger rotors in references 3 and 4 for similar ranges of variables. However, the range of variables for the model tests included both autorotative and powered-flight conditions which permitted tests to extend well into the stall region. Inasmuch as the effects of the additional range of variables are believed to be of interest, a few samples of the double-amplitude flapping results are presented in figures 21 to 24.

A sample of the data which shows the typical effect of collective pitch angle is given in figure 21. (The short vertical lines are used again to designate the value of μ where stall effects are expected to become significant.) The effect of rotor angle of attack is illustrated by figure 22. Both figures show, in general, a consistent and rather

sharp increase in the flapping angle as the tip-speed ratio exceeds the value at which stall effects are expected to become important.

As shown in figure 23, the data obtained in this investigation do not show any definite effect of the amount of flapping-hinge offset on blade flapping. This fact is contrary to the results of reference 15 wherein the flapping was found to decrease when the flapping-hinge offset was moved from $e/R = 0$ to $e/R = 0.13$. However, flight conditions were somewhat different in the reference tests than those covered herein, particularly in that those results were obtained from tests conducted at a negative rotor angle of attack and over a much wider range of tip-speed ratios.

Comparison with theory.- In an effort to obtain a qualitative evaluation of the agreement between the trends obtained in the present experimental study and those predicted by simplified theoretical means, the first two harmonic components of the blade flapping angles were computed for collective pitch angles of 3° and 6° and rotor angles of attack of 0° and 20°. Both the experimental results (all harmonics) and the calculated results (first two harmonics) are given in figure 24. The calculated results are based on the assumptions that the blades do not stall, that the induced velocity is uniform over the rotor disk, and that λ^2 is relatively small compared with μ^2. With these assumptions on inflow conditions and stall, the value of λ was calculated by the method of reference 5 and used to obtain the effective angles of attack of the blade segments and the resulting flapping angles.

A comparison of the results presented in figure 24 shows that the experimental flapping angles generally exceed the calculated angles. For $\alpha = 0^\circ$, this discrepancy is most pronounced at low values of μ, but for $\alpha = 20^\circ$, significant differences are apparent at both the higher and lower values of μ. The results of the calculations showed that the assumption of uniform inflow essentially leads to pure first-harmonic flapping, the magnitudes of the second harmonic components being comparatively negligible. This was true for both $\alpha = 0^\circ$ and $\alpha = 20^\circ$. Furthermore, for $\theta = 3^\circ$ or 6° and $\alpha = 0^\circ$, the calculated lateral flapping is negligible compared with the longitudinal flapping. For $\theta = 3^\circ$ or 6° and $\alpha = 20^\circ$, the ratio of longitudinal flapping to lateral flapping decreases monotonically from a value of approximately 3 at $\mu = 0.04$ to 2 at $\mu = 0.22$.

The fact that the experimental values of $\bar{\beta}$ as shown in figure 24 are substantially higher at the lower values of μ than the calculated values is probably due to asymmetric inflow distributions over the rotor, and it is expected that such inflow conditions could lead to a considerable amount of lateral flapping. (See refs. 3 and 16.) The existence of blade stall at the higher values of μ would be expected to result

in increased flapping as indicated by the high experimental values shown in figure 24(b).

CONCLUDING REMARKS

The results of a wind-tunnel investigation of the blade bending moments and flapping angles for a two-blade rotor having a diameter of 4 feet and a solidity of 0.037 and tested at positive rotor angles of attack may be summarized by the following remarks.

The double amplitude of periodic bending moments of the blade generally increase with tip-speed ratio up to a tip-speed ratio within the transition region. Above this value, the bending moments decrease for a range of tip-speed ratio and then increase sharply with further increases in tip-speed ratio. The tip-speed ratio corresponding to the peak value of bending moment is a function of rotor angle of attack and generally decreases as the angle of attack is increased. At the higher values of tip-speed ratio, above the point of transition, the blade bending moment increases substantially with blade collective pitch angle and rotor angle of attack. Below the transition range, the effect of these variables depends on the configuration of variables being studied.

A study of the spanwise distribution of the periodic bending moments indicates that the use of a flapping hinge does not appreciably affect the bending moments over the outer half of the blade but, as expected, the reduction over the inboard half is substantial. This reduction in bending moment appears to be significantly greater at higher tip-speed ratios than at lower tip-speed ratios. The data for the flapping configurations also show a general reduction in bending moment as the offset of the flapping hinge is increased.

The results of harmonic analyses of samples of the data show that the higher harmonic contributions to the total bending moments are appreciable, particularly in the transition range.

A study of the blade flapping angles shows that the results are in general agreement with the results previously found for larger autogiro rotors over compatible ranges of test variables. For conditions of rotor angle of attack and collective pitch angle which lead to substantial effects of stall, the flapping angles increase sharply with tip-speed ratio.

A comparison of the measured flapping angles with those calculated by means of simplified theory in which effects of asymmetric flow and blade stall are neglected shows good agreement at intermediate ranges of

tip-speed ratio but shows that the simplified theory greatly underestimates the flapping angles at low and at high values of tip-speed ratio if the rotor variables are such that significant stall effects are encountered.

Langley Research Center,
National Aeronautics and Space Administration,
Langley Field, Va., December 9, 1958.

REFERENCES

1. Glauert, H.: A General Theory of the Autogiro. R. & M. No. 1111, British A.R.C., 1926.

2. Lock, C. N. H.: Further Development of Autogyro Theory. Parts I and II. R. & M. No. 1127, British A.R.C., 1928.

3. Wheatley, John B.: An Aerodynamic Analysis of the Autogiro Rotor With a Comparison Between Calculated and Experimental Results. NACA Rep. 487, 1934.

4. Wheatley, John B., and Bioletti, Carlton: Wind-Tunnel Tests of 10-Foot-Diameter Autogiro Rotors. NACA Rep. 552, 1936.

5. Bailey, F. J., Jr.: A Simplified Theoretical Method of Determining the Characteristics of a Lifting Rotor in Forward Flight. NACA Rep. 716, 1941.

6. Hohenemser, Kurt H.: Remarks on the Unloaded Rotor Type of Convertiplane. Proc. Eleventh Annual Forum, Am. Helicopter Soc., Apr. 27-30, 1955, pp. 12-28.

7. Hohenemser, Kurt H.: Aerodynamic Aspects of the Unloaded Rotor Convertible Helicopter. Jour. Am. Helicopter Soc., vol. 2, no. 1, Jan. 1957, pp. 47-54.

8. Marks, Marvin D.: Flight Test Development of XV-1 Convertiplane. Jour. Am. Helicopter Soc., vol. 2, no. 1, Jan. 1957, pp. 55-63.

9. Daughaday, H., and Kline, J.: An Approach to the Determination of Higher Harmonic Rotor Blade Stresses. Proc. Ninth Annual Forum, Am. Helicopter Soc., Inc., May 14-17, 1953, pp. 90-126.

10. Meyer, John R., Jr.: An Investigation of Bending-Moment Distribution on a Model Helicopter Rotor Blade and a Comparison With Theory. NACA TN 2626, 1952.

11. McCarty, John Locke, and Brooks, George W.: A Dynamic-Model Study of the Effect of Added Weights and Other Structural Variations on the Blade Bending Strains of an Experimental Two-Blade Jet-Driven Helicopter in Hovering and Forward Flight. NACA TN 3367, 1955.

12. Yntema, Robert T.: Simplified Procedures and Charts for the Rapid Estimation of Bending Frequencies of Rotating Beams. NACA TN 3459, 1955. (Supersedes NACA RM L54G02.)

13. Gessow, Alfred, and Myers, Garry C., Jr.: Aerodynamics of the Helicopter. The MacMillan Co., c.1952.

14. Jacobs, Eastman N., and Sherman, Albert: Airfoil Section Characteristics As Affected by Variations of the Reynolds Number. NACA Rep. 586, 1937.

15. Meyer, John R., Jr., and Falabella, Gaetano, Jr.: An Investigation of the Experimental Aerodynamic Loading on a Model Helicopter Rotor Blade. NACA TN 2953, 1953.

16. Myers, Garry C., Jr.: Flight Measurements of Helicopter Blade Motion With a Comparison Between Theoretical and Experimental Results. NACA TN 1266, 1947.

TABLE I.- DOUBLE-AMPLITUDE BLADE FLAPPING AND BENDING-MOMENT DATA FOR FIXED-AT-ROOT CONFIGURATION

μ	$\alpha = 0^\circ$					$\alpha = 10^\circ$					$\alpha = 20^\circ$					$\alpha = 30^\circ$					$\alpha = 40^\circ$					$\alpha = 50^\circ$					$\alpha = 60^\circ$				
	$\bar{\beta}$	M_1	M_2	M_3	M_4	$\bar{\beta}$	M_1	M_2	M_3	M_4	$\bar{\beta}$	M_1	M_2	M_3	M_4	$\bar{\beta}$	M_1	M_2	M_3	M_4	$\bar{\beta}$	M_1	M_2	M_3	M_4	$\bar{\beta}$	M_1	M_2	M_3	M_4	$\bar{\beta}$	M_1	M_2	M_3	M_4
$\theta = 0^\circ$																																			
0.015		----	----	----	----		----	----	----	----		----	----	----	----		----	----	----	----		----	----	----	----		----	----	----	----		0.28	0.06	0.05	0.03
.03		0.23	0.08	0.13	0.09		0.42	0.14	0.17	0.12		0.42	0.17	0.14	0.07		0.40	0.12	0.13	0.09		0.28	0.08	0.08	0.06		0.24	0.06	0.06	0.05		.26	.08	.06	.04
.045		.20	.11	.16	.11		.36	.17	.19	.14		.43	.14	.17	.10		.42	.10	.07	.06		.39	.10	.07	.05		.45	.12	.09	.06		.53	.13	.12	.07
.06		.28	.12	.17	.11		.30	.17	.19	.14		.45	.13	.18	.12		.54	.13	.11	.07		.64	.16	.13	.07		.62	.17	.14	.08		.55	.13	.13	.10
.075		.28	.12	.16	.11		.46	.16	.19	.14		.47	.14	.16	.11		.59	.17	.15	.08		.71	.18	.17	.09		.67	.17	.16	.10		----	----	----	----
.09		.29	.11	.15	.10		.32	.15	.18	.13		.52	.16	.18	.11		.63	.19	.20	.10		.78	.19	.19	.11		.96	.18	.18	.13		----	----	----	----
.12		.30	.10	.13	.08		.42	.13	.18	.13		.64	.18	.23	.12		.94	.21	.26	.13		1.31	.20	.22	.15		----	----	----	----		----	----	----	----
.15		.32	.11	.12	.08		.58	.15	.20	.13		.86	.23	.27	.13		1.66	.30	.30	.17		----	----	----	----		----	----	----	----		----	----	----	----
.18		.34	.12	.14	.09		.80	.19	.23	.15		1.27	.31	.30	.15		----	----	----	----		----	----	----	----		----	----	----	----		----	----	----	----
.24		.44	.17	.19	.12		1.37	.32	.33	.19		3.20	.52	.41	.21		----	----	----	----		----	----	----	----		----	----	----	----		----	----	----	----
.30		.56	.23	.28	.16		2.22	.49	.46	.24		----	----	----	----		----	----	----	----		----	----	----	----		----	----	----	----		----	----	----	----
$\theta = 3^\circ$																																			
0.015		----	----	----	----		----	----	----	----		----	----	----	----		----	----	----	----		0.70	0.25	0.35	0.16		0.65	0.20	0.29	0.15		----	0.19	0.55	0.15
.03		0.44	0.15	0.21	----		0.76	0.18	0.29	0.25		1.03	0.26	0.47	0.35		1.02	0.36	0.36	0.21		1.04	.32	.35	.20		.62	.18	.22	.18		0.70	.16	.31	.13
.045		.68	.21	.27	0.21		1.01	.34	.42	.33		1.31	.40	.45	.36		1.00	.32	.34	.24		.45	.16	.19	.15		.60	.18	.15	.12		.69	.18	.30	.10
.06		.80	.25	.32	.26		1.20	.41	.46	.35		1.22	.36	.38	.31		.75	.22	.26	.20		.60	.17	.17	.13		.78	.21	.18	.12		.60	.10	.41	.14
.075		.90	.28	.36	.30		1.10	.38	.40	.30		.99	.31	.33	.25		.60	.17	.20	.15		.79	.20	.21	.14		.85	.20	.20	.13		----	----	----	----
.09		.98	.28	.38	.31		1.08	.35	.34	.26		.86	.28	.31	.20		.70	.18	.23	.15		1.00	.22	.23	.16		1.20	.15	.19	.19		----	----	----	----
.12		1.10	.30	.37	.28		1.10	.32	.31	.21		1.00	.27	.29	.18		1.30	.27	.30	.19		1.30	.22	----	.28		----	----	----	----		----	----	----	----
.15		1.20	.32	.33	.26		1.28	.32	.31	.19		1.40	.31	.32	.21		3.00	.51	.37	.30		----	----	----	----		----	----	----	----		----	----	----	----
.18		1.32	.34	.33	.25		1.50	.36	.32	.19		2.35	.46	.37	.28		----	----	----	----		----	----	----	----		----	----	----	----		----	----	----	----
.24		1.79	.44	.37	.28		2.65	.57	.40	.25		6.00	1.24	.51	.53		----	----	----	----		----	----	----	----		----	----	----	----		----	----	----	----
.30		2.70	.58	.52	.36		4.45	.90	.54	.33		----	----	----	----		----	----	----	----		----	----	----	----		----	----	----	----		----	----	----	----
$\theta = 6^\circ$																																			
0.015		----	----	----	----		----	----	----	----		----	----	----	----		----	----	----	----		----	----	----	----		0.50	----	0.42	0.42		0.74	0.21	0.33	0.28
.03		0.80	0.28	0.37	0.20		0.95	0.28	0.35	0.28		1.20	0.40	0.49	0.35		1.35	0.46	0.50	0.33		1.30	0.40	0.43	0.34		1.15	0.30	.35	.27		.60	.19	.21	.18
.045		1.15	.35	.39	.26		1.40	.43	.50	.37		1.89	.60	.65	.49		1.53	.47	.50	.32		.83	.26	.33	.27		.60	.18	.20	.20		.40	.17	.22	.21
.06		1.30	.40	.41	.31		1.80	.57	.69	.41		1.80	.56	.56	.43		1.15	.32	.40	.29		.50	.17	.28	.26		.80	.26	.24	.22		2.00	.53	.41	.39
.075		1.45	.44	.46	.33		1.85	.55	.61	.38		1.40	.46	.47	.36		.85	.25	.29	.27		.85	.24	.28	.27		1.12	.33	.29	.25		----	----	----	----
.09		1.60	.47	.51	.35		1.75	.50	.52	.34		1.20	.39	.41	.31		1.00	.26	.29	.29		1.75	.41	.36	.33		3.75	.77	.56	.49		----	----	----	----
.12		1.85	.49	.51	.36		1.80	.46	.44	.32		1.70	.51	.38	.35		2.75	.64	.43	.42		5.00	.95	.76	.65		----	----	----	----		----	----	----	----
.15		2.15	.51	.52	.35		2.20	.49	.41	.35		3.55	.81	.51	.49		5.10	1.03	.71	.62		----	----	----	----		----	----	----	----		----	----	----	----
.18		2.55	.57	.52	.35		3.25	.67	.50	.41		5.10	1.07	.75	.64		----	----	----	----		----	----	----	----		----	----	----	----		----	----	----	----
.24		3.35	.75	.47	.40		5.55	1.10	.82	.61		7.65	1.41	1.22	.99		----	----	----	----		----	----	----	----		----	----	----	----		----	----	----	----
.30		5.10	.98	.75	.52		7.30	1.34	1.09	.84		----	----	----	----		----	----	----	----		----	----	----	----		----	----	----	----		----	----	----	----

TABLE II.- DOUBLE-AMPLITUDE BLADE FLAPPING AND BENDING-MOMENT DATA FOR FLAPPING CONFIGURATION WITH e/R = 0

μ	α = 0°					α = 10°					α = 20°					α = 30°					α = 40°					α = 50°					α = 60°				
	$\bar{\beta}$	M_1	M_2	M_3	M_4	$\bar{\beta}$	M_1	M_2	M_3	M_4	$\bar{\beta}$	M_1	M_2	M_3	M_4	$\bar{\beta}$	M_1	M_2	M_3	M_4	$\bar{\beta}$	M_1	M_2	M_3	M_4	$\bar{\beta}$	M_1	M_2	M_3	M_4	$\bar{\beta}$	M_1	M_2	M_3	M_4
θ = 0°																																			
0.015	-----	----	----	----	----	-----	----	----	----	----	-----	----	----	----	----	-----	----	----	----	----	----	----	----	----	----	0.88	0.10	0.05	0.08	0.04	0.58	0.07	0.04	0.04	0.05
.03	0.81	0.10	0.06	0.10	0.10	0.82	0.19	0.10	0.11	----	0.60	0.27	0.15	0.16	0.11	0.50	0.24	0.12	0.17	0.08	0.70	0.11	0.06	0.07	0.06	.55	.07	.04	.05	.04	.70	.10	.04	.05	.04
.045	.75	.19	.11	.14	.12	.83	.23	.14	.17	.14	.75	.27	.14	.18	.13	.58	.15	.08	.10	.10	.55	.09	.06	.08	.07	1.08	.10	.05	.07	.05	1.28	.11	.06	.08	.06
.06	.70	.23	.12	.16	.13	.82	.24	.16	.19	.17	.80	.22	.13	.19	.17	.55	.12	.08	.10	.11	.60	.11	.07	.11	.08	1.05	.12	.07	.11	.07	1.05	.11	.07	.11	.07
.075	.65	.23	.13	.16	.12	.85	.24	.16	.20	.16	.80	.20	.12	.19	.16	.50	.14	.11	.13	.11	.85	.14	.10	.13	.10	.85	.13	.08	.12	.08	-----	-----	-----	-----	-----
.09	.65	.24	.13	.15	.11	.82	.25	.16	.20	.15	.80	.22	.13	.19	.13	.55	.18	.14	.16	.12	.65	.20	.13	.16	.11	----	.20	.09	.18	.10	-----	-----	-----	-----	-----
.12	.64	.24	.13	.15	.10	.85	.27	.15	.20	.15	.85	.27	.15	.19	.12	1.05	.27	.18	.21	.12	2.80	.36	.17	.21	.14	----	----	----	----	----	-----	-----	-----	-----	-----
.15	.63	.24	.13	.15	.10	.87	.29	.16	.20	.15	1.50	.31	.18	.21	.11	2.47	.35	.22	.25	.15	----	----	----	----	----	----	----	----	----	----	-----	-----	-----	-----	-----
.18	.65	.25	.14	.15	.12	1.00	.33	.17	.20	.16	2.45	.37	.21	.23	.13	-----	.43	.26	.31	.20	----	----	----	----	----	----	----	----	----	----	-----	-----	-----	-----	-----
.24	.76	.30	.17	.17	.16	2.42	.41	.20	.22	.18	5.35	.48	.27	.31	.21	-----	----	----	----	----	----	----	----	----	----	----	----	----	----	----	-----	-----	-----	-----	-----
.30	1.10	.39	.20	.21	.21	4.00	.51	.23	.24	.22	-----	----	----	----	----	-----	----	----	----	----	----	----	----	----	----	----	----	----	----	----	-----	-----	-----	-----	-----
θ = 3°																																			
0.015	-----	----	----	----	----	-----	----	----	----	----	-----	----	----	----	----	-----	----	----	----	----	1.50	0.44	0.26	0.35	----	1.63	0.32	0.15	----	0.26	0.90	0.28	0.15	0.23	0.19
.03	0.80	----	----	----	0.20	1.60	----	0.21	0.30	----	1.90	0.45	0.23	0.31	0.29	2.40	0.49	0.24	0.29	0.21	2.30	.39	.17	.29	0.24	2.30	.34	.14	0.32	.28	1.50	.27	.12	.18	.15
.045	1.13	0.37	0.19	0.31	.27	2.13	0.57	.27	.42	0.37	2.40	.71	.27	.49	.42	1.95	.45	.18	.27	.21	1.45	.34	.15	.25	.22	2.27	.31	.14	.30	.24	1.95	.28	.13	.15	.12
.06	1.60	.50	.24	.35	.27	2.40	.63	.28	.44	.39	2.50	.66	.25	.39	.36	1.40	.39	.16	.24	.19	1.40	.34	.17	.24	.21	2.20	.32	.15	.30	.23	1.40	.33	.17	.21	.20
.075	1.90	.55	.27	.36	.25	2.40	.58	.28	.37	.33	1.95	.55	.22	.35	.27	1.37	.37	.16	.22	.18	1.80	.36	.19	.24	.20	2.20	.34	.16	.31	.25	-----	-----	-----	-----	-----
.09	2.10	.56	.26	.33	.23	2.45	.52	.27	.30	.27	2.00	.46	.21	.32	.23	1.80	.37	.17	.22	.19	2.60	.40	.21	.26	.22	5.70	.40	.20	.38	.34	-----	-----	-----	-----	-----
.12	2.50	.53	.28	.28	.22	2.65	.45	.25	.26	.21	2.60	.41	.21	.28	.19	3.70	.42	.22	.23	.21	7.60	.51	.27	.30	.29	-----	-----	-----	-----	-----	-----	-----	-----	-----	-----
.15	3.20	.50	.27	.26	.22	3.20	.44	.24	.24	.18	3.70	.45	.24	.29	.19	9.10	.51	.28	.27	.26	-----	.66	-----	-----	-----	-----	-----	-----	-----	-----	-----	-----	-----	-----	-----
.18	3.55	.53	.25	.25	.24	4.30	.47	.23	.26	.18	7.30	.53	.31	.38	.26	-----	----	----	----	----	----	----	----	----	----	----	----	----	----	----	-----	-----	-----	-----	-----
.24	4.20	.62	.27	.25	.30	7.20	.58	.27	.42	.31	13.50	.76	.54	.72	.51	-----	----	----	----	----	----	----	----	----	----	----	----	----	----	----	-----	-----	-----	-----	-----
.30	6.30	.73	.31	.27	.36	12.00	.81	.38	.67	.49	-----	----	----	----	----	-----	----	----	----	----	----	----	----	----	----	----	----	----	----	----	-----	-----	-----	-----	-----
θ = 6°																																			
0.015	-----	----	----	----	----	-----	----	----	----	----	-----	----	----	----	----	-----	----	----	----	----	----	----	----	----	----	1.15	----	0.33	----	0.28	1.20	0.35	0.19	0.30	0.25
.03	2.00	----	----	----	----	1.00	----	----	----	----	2.50	0.49	0.28	0.38	0.19	3.20	0.70	0.33	0.46	0.28	3.80	0.56	0.28	0.30	0.19	2.10	0.46	.22	0.33	.27	.90	.35	.16	.22	.19
.045	2.60	----	----	0.35	0.17	3.88	0.62	0.30	0.44	0.26	4.20	.82	.34	.51	.31	4.45	.70	.27	.42	.25	1.85	.48	.21	.30	.21	.90	.34	.23	.26	.24	1.65	.36	.20	.26	.24
.06	3.20	0.55	0.28	.38	.19	4.60	.80	.35	.53	.33	4.50	.94	.34	.57	.34	2.70	.51	.20	.35	.22	1.20	.45	.24	.31	.22	1.60	.39	.27	.28	.24	4.30	.50	.27	.33	.35
.075	3.70	.60	.32	.37	.19	4.60	.85	.36	.52	.33	3.45	.86	.30	.48	.29	2.40	.46	.19	.29	.22	2.47	.47	.26	.31	.23	3.30	.46	.29	.32	.26	8.40	.69	.38	.42	-----
.09	4.05	.63	.33	.37	.18	4.20	.83	.36	.48	.29	3.00	.73	.27	.38	.25	3.30	.51	.22	.32	.23	5.00	.54	.28	.35	.27	9.50	.80	.37	.48	.39	-----	-----	-----	-----	-----
.12	4.75	.66	.33	.35	.17	4.40	.76	.36	.42	.25	4.60	.65	.29	.36	.25	8.00	.70	.35	.46	.31	-----	----	.29	.50	.40	-----	-----	-----	-----	-----	-----	-----	-----	-----	-----
.15	5.40	.66	.33	.35	.18	5.50	.70	.37	.41	.24	9.10	.67	.36	.44	.31	13.90	.94	.58	.63	.44	-----	----	----	----	----	-----	-----	-----	-----	-----	-----	-----	-----	-----	-----
.18	6.30	.68	.33	.37	.20	7.90	.69	.39	.44	.26	12.90	.74	.44	.56	.38	-----	----	----	----	----	----	----	----	----	----	-----	-----	-----	-----	-----	-----	-----	-----	-----	-----
.24	8.80	.75	.34	.43	.26	13.60	.70	.45	.57	.33	-----	.99	----	.82	.56	-----	----	----	----	----	----	----	----	----	----	-----	-----	-----	-----	-----	-----	-----	-----	-----	-----
.30	12.40	.89	.36	.53	.34	17.30	.76	.53	.72	.42	-----	----	----	----	----	-----	----	----	----	----	----	----	----	----	----	-----	-----	-----	-----	-----	-----	-----	-----	-----	-----

TABLE III.- DOUBLE-AMPLITUDE BLADE FLAPPING AND BENDING-MOMENT DATA FOR FLAPPING CONFIGURATION WITH $e/R = 0.05$

μ	$\alpha = 0°$					$\alpha = 10°$					$\alpha = 20°$					$\alpha = 30°$					$\alpha = 40°$					$\alpha = 50°$					$\alpha = 60°$				
	$\bar{\beta}$	M_1	M_2	M_3	M_4	$\bar{\beta}$	M_1	M_2	M_3	M_4	$\bar{\beta}$	M_1	M_2	M_3	M_4	$\bar{\beta}$	M_1	M_2	M_3	M_4	$\bar{\beta}$	M_1	M_2	M_3	M_4	$\bar{\beta}$	M_1	M_2	M_3	M_4	$\bar{\beta}$	M_1	M_2	M_3	M_4
$\theta = 0°$																																			
0.015	-----	----	----	----	----	-----	----	----	----	----	-----	----	----	----	----	-----	----	----	----	----	-----	----	----	----	----	-----	----	----	0.03	----	0.35	0.06	0.03	0.02	0.02
.03	0.75	0.06	0.04	0.06	0.07	1.25	0.10	0.05	0.09	0.08	0.75	0.10	0.08	0.12	0.10	0.65	0.10	0.06	0.05	0.05	1.13	0.08	0.05	0.05	0.05	1.20	0.06	0.03	.05	0.04	1.95	.06	.04	.05	.03
.045	.78	.11	.06	.09	.09	1.06	.12	.08	.11	.10	.75	.14	.10	.10	.08	.95	.07	.05	.08	.06	1.10	.06	.05	.07	.06	1.28	.06	.06	.07	.06	2.07	.07	.06	.09	.06
.06	.85	.14	.07	.11	.09	.98	.12	.10	.13	.10	.90	.11	.07	.10	.08	1.20	.08	.07	.10	.08	1.23	.07	.07	.09	.07	2.40	.07	.07	.09	.06	2.30	.09	.06	.09	.07
.075	.88	.14	.09	.12	.09	1.00	.12	.10	.14	.10	1.18	.11	.08	.12	.09	1.40	.10	.08	.11	.09	1.75	.10	.08	.11	.08	2.90	.06	.07	.10	.07		----	----	----	----
.09	.90	.14	.09	.12	.09	1.10	.14	.11	.15	.10	1.09	.13	.09	.13	.10	1.60	.12	.09	.12	.09	1.86	.13	.09	.13	.08	-----	.13	.09	.15	.11	----	----	----	----	----
.12	.90	.16	.09	.12	.08	1.35	.18	.11	.16	.10	1.59	.17	.10	.14	.10	1.95	.15	.11	.15	.09	----	----	----	----	----	-----	----	----	----	----	----	----	----	----	----
.15	.97	.17	.09	.13	.09	1.56	.21	.11	.17	.11	2.06	.19	.12	.15	.10	2.25	.18	.13	.18	.11	----	----	----	----	----	-----	----	----	----	----	----	----	----	----	----
.18	1.10	.19	.10	.14	.10	1.65	.23	.12	.17	.12	2.20	.22	.14	.16	.10	-----	----	----	----	----	----	----	----	----	----	-----	----	----	----	----	----	----	----	----	----
.24	1.20	.26	.12	.15	.13	1.75	.27	.13	.18	.14	2.10	.31	.18	.25	.18	-----	----	----	----	----	----	----	----	----	----	-----	----	----	----	----	----	----	----	----	----
.30	1.17	.38	.18	.17	.14	1.80	.32	.14	.20	.14	-----	----	----	----	----	-----	----	----	----	----	----	----	----	----	----	-----	----	----	----	----	----	----	----	----	----
$\theta = 3°$																																			
0.015	-----	----	----	----	----	-----	----	----	----	----	-----	----	----	----	----	-----	----	----	----	----	----	----	----	----	0.13	2.50	0.20	0.13	0.17	0.13	2.60	0.18	0.11	0.12	0.13
.03	2.05	----	0.15	0.32	0.25	3.50	0.23	0.18	0.31	0.25	4.40	0.38	0.25	0.27	0.25	6.70	0.33	0.20	0.26	0.23	4.83	0.26	0.13	0.20	.17	3.50	.22	.11	.17	.15	3.30	.14	.08	.11	.12
.045	2.20	0.22	.17	.32	.25	3.90	.47	.29	.37	.35	4.33	.47	.26	.38	.34	6.35	.28	.16	.23	.20	3.15	.23	.12	.18	.15	1.95	.19	.13	.15	.13	3.50	.14	.10	.13	.11
.06	2.30	.32	.21	.31	.23	3.80	.47	.29	.37	.33	4.30	.42	.24	.31	.27	5.10	.21	.12	.20	.17	3.40	.23	.13	.18	.14	3.75	.17	.12	.15	.12	----	.25	.14	.18	.15
.075	2.38	.38	.24	.30	.23	3.70	.40	.25	.33	.26	4.30	.38	.21	.27	.25	4.20	.21	.13	.19	.16	4.58	.23	.16	.20	.16	4.95	.21	.12	.17	.14		----	----	----	----
.09	2.40	.41	.24	.29	.22	3.70	.36	.23	.28	.23	4.30	.34	.19	.25	.22	5.20	.24	.17	.22	.16	6.10	.29	.20	.23	.17	8.90	.29	.17	.21	.22	----	----	----	----	----
.12	2.30	.41	.23	.28	.22	3.80	.36	.21	.24	.21	4.60	.29	.19	.24	.18	8.05	.33	.21	.26	.19	----	----	----	----	----	-----	----	----	----	----	----	----	----	----	----
.15	2.35	.42	.23	.27	.23	4.33	.35	.21	.21	.16	5.55	.31	.20	.25	.22	13.20	.44	.23	.28	.36	----	----	----	----	----	-----	----	----	----	----	----	----	----	----	----
.18	2.30	.43	.25	.26	.26	5.28	.33	.22	.21	.16	8.00	.39	.23	.29	.29	-----	----	----	----	----	----	----	----	----	----	-----	----	----	----	----	----	----	----	----	----
.24	3.30	.47	.27	.29	.28	8.18	.34	.24	.32	.28	16.20	.67	.51	----	.47	-----	----	----	----	----	----	----	----	----	----	-----	----	----	----	----	----	----	----	----	----
.30	4.88	.51	.22	.27	.26	11.50	.47	.27	.43	.38	-----	----	----	----	----	-----	----	----	----	----	----	----	----	----	----	-----	----	----	----	----	----	----	----	----	----
$\theta = 6°$																																			
0.015	-----	----	----	----	----	-----	----	----	----	----	-----	----	----	----	----	-----	----	----	----	----	----	----	----	----	----	2.00	----	----	----	----	3.70	0.36	0.20	0.26	0.22
.03	3.40	----	----	----	----	4.00	0.23	0.18	0.34	0.30	6.00	0.32	0.23	0.33	0.33	7.50	0.40	0.27	0.31	0.30	6.00	0.41	0.21	0.28	0.25	5.90	0.31	0.18	0.26	0.24	4.00	.25	.14	.21	.20
.045	4.20	0.25	0.20	0.33	0.31	5.30	.44	.26	.37	.36	6.80	.56	.31	.38	.38	6.80	.44	.21	.34	.29	4.85	.25	.13	.25	.24	5.20	.27	.17	.21	.20	4.70	.29	.19	.21	.15
.06	4.90	.45	.27	.37	.30	6.20	.59	.34	.41	.40	7.00	.51	.22	.36	.33	4.70	.34	.16	.28	.24	4.40	.38	.21	.25	.26	5.85	.29	.20	.20	.17	8.80	.42	.22	.25	.27
.075	5.50	.54	.31	.36	.29	6.70	.61	.34	.40	.40	7.20	.46	.20	.33	.31	3.90	.32	.14	.27	.23	5.85	.31	.18	.24	.28	7.20	.32	.20	.20	.23	----	----	----	----	----
.09	5.90	.58	.33	.35	.31	7.00	.56	.32	.37	.36	7.20	.41	.20	.28	.31	7.30	.36	.14	.28	.27	8.10	.33	.17	.24	.29	11.85	.59	.33	.57	.33	----	----	----	----	----
.12	6.55	.60	.32	.34	.31	7.20	.40	.27	.31	.29	8.50	.38	.23	.29	.27	12.80	.44	.26	.39	.33	----	----	----	----	----	-----	----	----	----	----	----	----	----	----	----
.15	6.90	.57	.32	.35	.26	7.30	.43	.23	.29	.24	11.30	.44	.28	.40	.32	15.80	.51	.34	.49	.48	----	----	----	----	----	-----	----	----	----	----	----	----	----	----	----
.18	7.20	.54	.29	.34	.28	9.00	.51	.23	.34	.31	14.95	.52	.31	.52	.43	-----	----	----	----	----	----	----	----	----	----	-----	----	----	----	----	----	----	----	----	----
.24	8.75	.59	.32	.35	.38	14.85	.70	.30	.60	.48	23.40	.63	.36	.68	----	-----	----	----	----	----	----	----	----	----	----	-----	----	----	----	----	----	----	----	----	----
.30	13.30	.66	.21	.38	.38	18.90	.61	.30	.62	.54	-----	----	----	----	----	-----	----	----	----	----	----	----	----	----	----	-----	----	----	----	----	----	----	----	----	----

TABLE IV.- DOUBLE-AMPLITUDE BLADE FLAPPING AND BENDING-MOMENT DATA FOR FLAPPING CONFIGURATION WITH e/R = 0.10

μ	$\alpha = 0^\circ$					$\alpha = 10^\circ$					$\alpha = 20^\circ$					$\alpha = 30^\circ$					$\alpha = 40^\circ$					$\alpha = 50^\circ$					$\alpha = 60^\circ$				
	$\bar{\beta}$	M_1	M_2	M_3	M_4	$\bar{\beta}$	M_1	M_2	M_3	M_4	$\bar{\beta}$	M_1	M_2	M_3	M_4	$\bar{\beta}$	M_1	M_2	M_3	M_4	$\bar{\beta}$	M_1	M_2	M_3	M_4	$\bar{\beta}$	M_1	M_2	M_3	M_4	$\bar{\beta}$	M_1	M_2	M_3	M_4
$\theta = 0^\circ$																																			
0.015	-----	----	----	----	----	-----	----	----	----	----	-----	----	----	----	----	-----	----	----	----	----	----	----	----	----	----	-----	----	----	----	----	3.75	0.05	0.05	0.04	0.04
.03	-----	0.06	0.05	0.10	0.08	2.40	----	----	0.15	0.11	3.10	----	0.09	0.09	0.08	3.90	0.10	0.06	0.06	0.06	3.90	0.08	0.05	0.06	0.04	3.70	0.06	0.05	0.05	0.03	3.90	.08	.06	.06	.04
.045	-----	.08	.05	.09	.07	2.83	0.14	0.12	.15	.10	3.40	0.15	.12	.13	.10	3.55	.09	.07	.08	.08	3.62	.08	.07	.08	.06	3.45	.07	.06	.07	.05	2.95	.10	.08	.11	.06
.06	-----	.10	.06	.10	.07	3.10	.11	.10	.15	.10	3.50	.09	.10	.13	.10	3.20	.09	.08	.11	.09	3.40	.09	.09	.11	.08	3.70	.09	.08	.12	.08	-----	.11	.10	.16	.07
.075	-----	.10	.08	.10	.06	3.18	.10	.10	.16	.11	3.65	.10	.09	.13	.10	3.35	.10	.10	.13	.10	3.37	.10	.10	.13	.09	3.35	.10	.09	.14	.09	-----	----	----	----	----
.09	-----	.11	.09	.11	.07	3.30	.10	.10	.16	.12	3.70	.09	.09	.14	.09	3.90	.11	.11	.16	.10	3.70	.11	.10	.15	.10	-----	.14	.09	----	----	-----	----	----	----	----
.12	-----	.11	.10	.12	.07	3.30	.12	.11	.17	.13	3.70	.10	.10	.14	.09	4.60	.15	.13	.19	.09	5.20	.12	.10	.18	.12	-----	----	----	----	----	-----	----	----	----	----
.15	-----	.12	.10	.13	.08	3.30	.15	.11	.17	.13	3.70	.14	.12	.15	.10	4.40	.16	.14	.22	.13	-----	----	----	----	----	-----	----	----	----	----	-----	----	----	----	----
.18	-----	.13	.11	.13	.09	3.50	.15	.11	.18	.14	3.70	.17	.15	.19	.11	-----	----	----	----	----	----	----	----	----	----	-----	----	----	----	----	-----	----	----	----	----
.24	-----	.15	.14	.13	.09	4.60	.24	.14	.23	.15	8.00	.21	.20	.33	.19	-----	----	----	----	----	----	----	----	----	----	-----	----	----	----	----	-----	----	----	----	----
.30	-----	.27	.18	.16	.14	6.70	.34	.20	.30	.18	-----	----	----	----	----	-----	----	----	----	----	----	----	----	----	----	-----	----	----	----	----	-----	----	----	----	----
$\theta = 3^\circ$																																			
0.015	-----	----	----	----	----	-----	----	----	----	----	-----	----	----	----	----	-----	----	----	----	----	3.80	----	0.22	0.31	0.19	4.55	0.21	0.17	0.20	0.10	5.80	0.19	0.11	0.16	----
.03	4.20	0.18	0.14	0.28	0.18	4.20	----	----	0.31	0.21	4.00	0.40	0.34	0.37	0.27	3.40	0.31	0.25	0.30	0.22	4.10	0.18	.13	.16	.15	5.10	.16	.12	.13	.12	5.60	.16	.09	.10	0.10
.045	3.60	.24	.18	.32	.20	4.20	0.40	0.33	.40	.27	4.60	.44	.32	.39	.31	3.95	.30	.16	.23	.22	4.20	.15	.12	.16	.14	4.60	.15	.11	.14	.10	4.60	.15	.11	.13	.11
.06	3.10	.29	.21	.34	.23	3.60	.45	.34	.37	.28	3.30	.34	.22	.29	.25	4.70	.19	.13	.18	.15	3.10	.15	.12	.18	.16	4.00	.15	.12	.17	.12	3.80	.18	.14	.20	.19
[illegible]	[illegible]	[illegible]	[illegible]	[illegible]	[illegible]	[illegible]	[illegible]	[illegible]	[illegible]	[illegible]	[illegible]	[illegible]	[illegible]	[illegible]	[illegible]	4.00	.16	.14	.21	.16	3.80	.16	.13	.21	.17	4.10	.16	.13	.18	.13	-----	----	----	----	----
.09	2.80	.37	.25	.34	.22	3.60	.36	.27	.35	.24	3.40	.24	.15	.22	.20	3.80	.17	.17	.23	.18	[illegible]	[illegible]	[illegible]	[illegible]	[illegible]	9.80	[illegible]	[illegible]	[illegible]	[illegible]	[illegible]	[illegible]	[illegible]	[illegible]	[illegible]
.12	3.10	.40	.25	.31	.21	4.20	.29	.25	.28	.20	4.70	.21	.18	.23	.15	5.50	.23	.21	.27	.19	-----	.20	.20	.29	----	-----	----	----	----	----	-----	----	----	----	----
.15	3.60	.39	.24	.28	.20	5.30	.26	.22	.26	.17	7.20	.21	.21	.27	.20	11.90	.45	.25	.29	.39	-----	----	----	----	----	-----	----	----	----	----	-----	----	----	----	----
.18	4.50	.39	.25	.29	.22	6.90	.25	.20	.29	.17	11.00	.28	.27	.34	.27	-----	----	----	----	----	-----	----	----	----	----	-----	----	----	----	----	-----	----	----	----	----
.24	7.00	.42	.27	.33	.23	10.60	.24	.19	.31	.22	-----	----	----	----	----	-----	----	----	----	----	-----	----	----	----	----	-----	----	----	----	----	-----	----	----	----	----
.30	9.70	.57	.26	.32	.20	14.10	.24	.24	.32	.29	-----	----	----	----	----	-----	----	----	----	----	-----	----	----	----	----	-----	----	----	----	----	-----	----	----	----	----
$\theta = 6^\circ$																																			
0.015	-----	----	----	----	----	-----	----	----	----	----	-----	----	----	----	----	-----	----	----	----	----	----	----	----	----	----	----	----	----	----	----	9.45	0.26	0.23	0.32	0.22
.03	3.20	0.18	----	0.36	0.39	-----	----	----	0.32	----	6.70	----	----	0.36	----	9.40	0.30	0.31	0.36	0.29	6.70	0.31	0.24	0.33	0.26	6.80	0.34	0.15	0.22	0.20	6.90	.26	.13	.17	.17
.045	3.90	.23	0.20	.39	.34	10.00	0.39	0.35	.40	0.35	6.78	0.55	0.42	.47	0.48	7.92	.37	.29	.40	.34	6.30	.26	.16	.23	.21	4.25	.19	.12	.18	.19	5.95	.24	.14	.20	.19
.06	4.30	.28	.28	.40	.31	5.50	.57	.44	.46	.45	7.00	.55	.37	.50	.46	7.40	.28	.17	.31	.27	5.80	.20	.14	.21	.20	4.20	.21	.15	.22	.21	11.20	.38	.24	.31	.29
.075	4.40	.39	.33	.39	.31	3.50	.58	.44	.47	.45	7.48	.49	.28	.43	.36	7.33	.24	.16	.26	.22	6.17	.21	.17	.22	.22	6.95	.24	.18	.25	.24	-----	----	----	----	----
.09	4.40	.47	.36	.38	.32	3.40	.48	.38	.44	.40	8.10	.43	.22	.36	.33	7.70	.26	.18	.27	.22	9.80	.31	.22	.27	.27	13.10	.45	.38	.50	.47	-----	----	----	----	----
.12	5.20	.54	.35	.38	.35	4.10	.37	.31	.37	.31	8.10	.35	.20	.32	.31	11.10	.40	.28	.38	.30	-----	----	.39	----	----	-----	----	----	----	----	-----	----	----	----	----
.15	6.30	.47	.30	.37	.39	6.00	.30	.27	.30	.28	11.40	.37	.28	.36	.32	17.60	.59	.37	.59	.56	-----	----	----	----	----	-----	----	----	----	----	-----	----	----	----	----
.18	7.40	.42	.29	.37	.42	10.40	.36	.29	.35	.34	15.00	.48	.37	.50	.43	-----	----	----	----	----	----	----	----	----	----	-----	----	----	----	----	-----	----	----	----	----
.24	9.60	.47	.32	.36	.46	13.10	.64	.38	.58	.52	17.60	----	.41	----	----	-----	----	----	----	----	----	----	----	----	----	-----	----	----	----	----	-----	----	----	----	----
.30	12.10	.56	.27	.35	.34	16.70	.68	.39	.65	.64	-----	----	----	----	----	-----	----	----	----	----	----	----	----	----	----	-----	----	----	----	----	-----	----	----	----	----

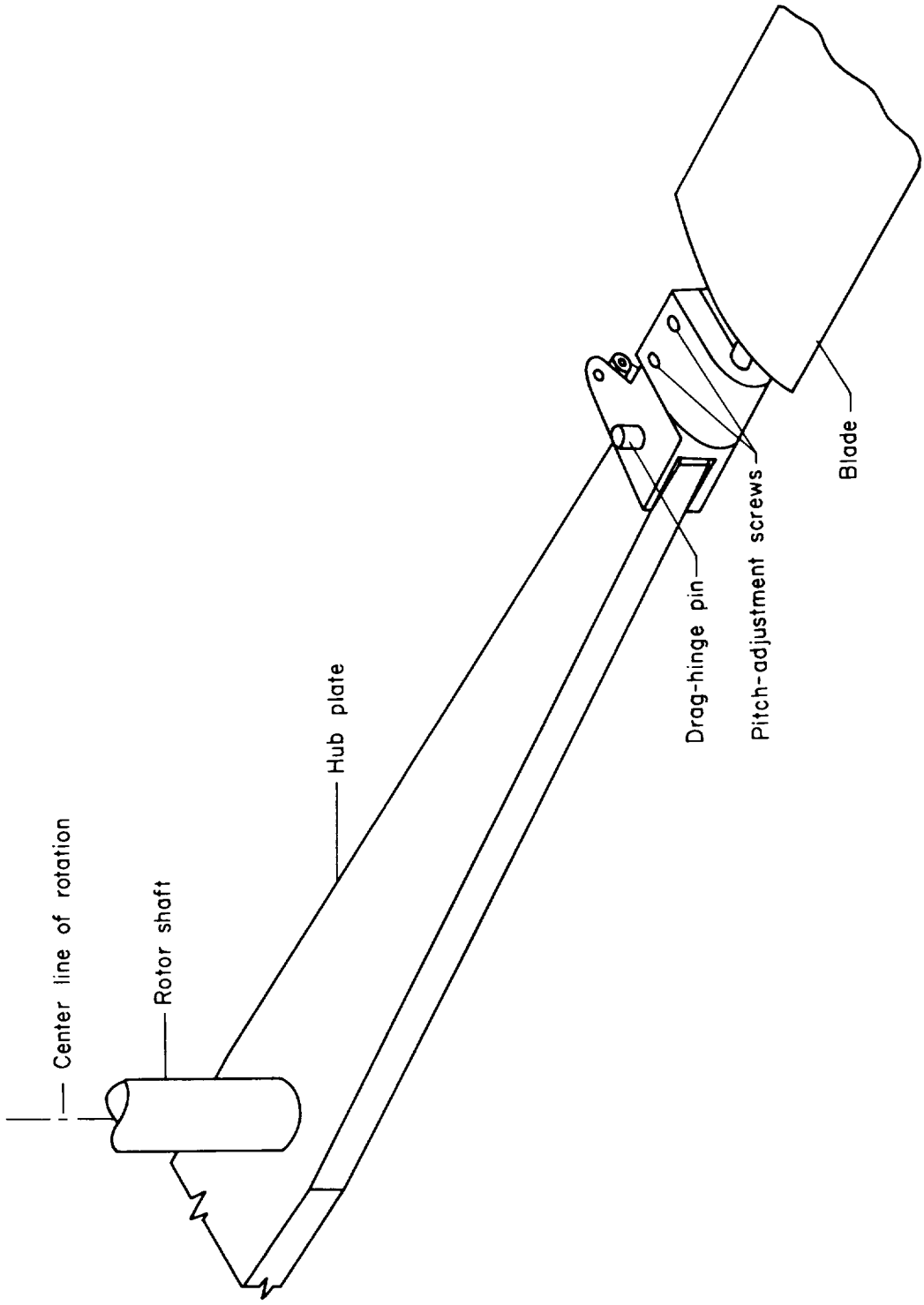

Figure 1.- Blade root fitting for fixed-at-root configuration.

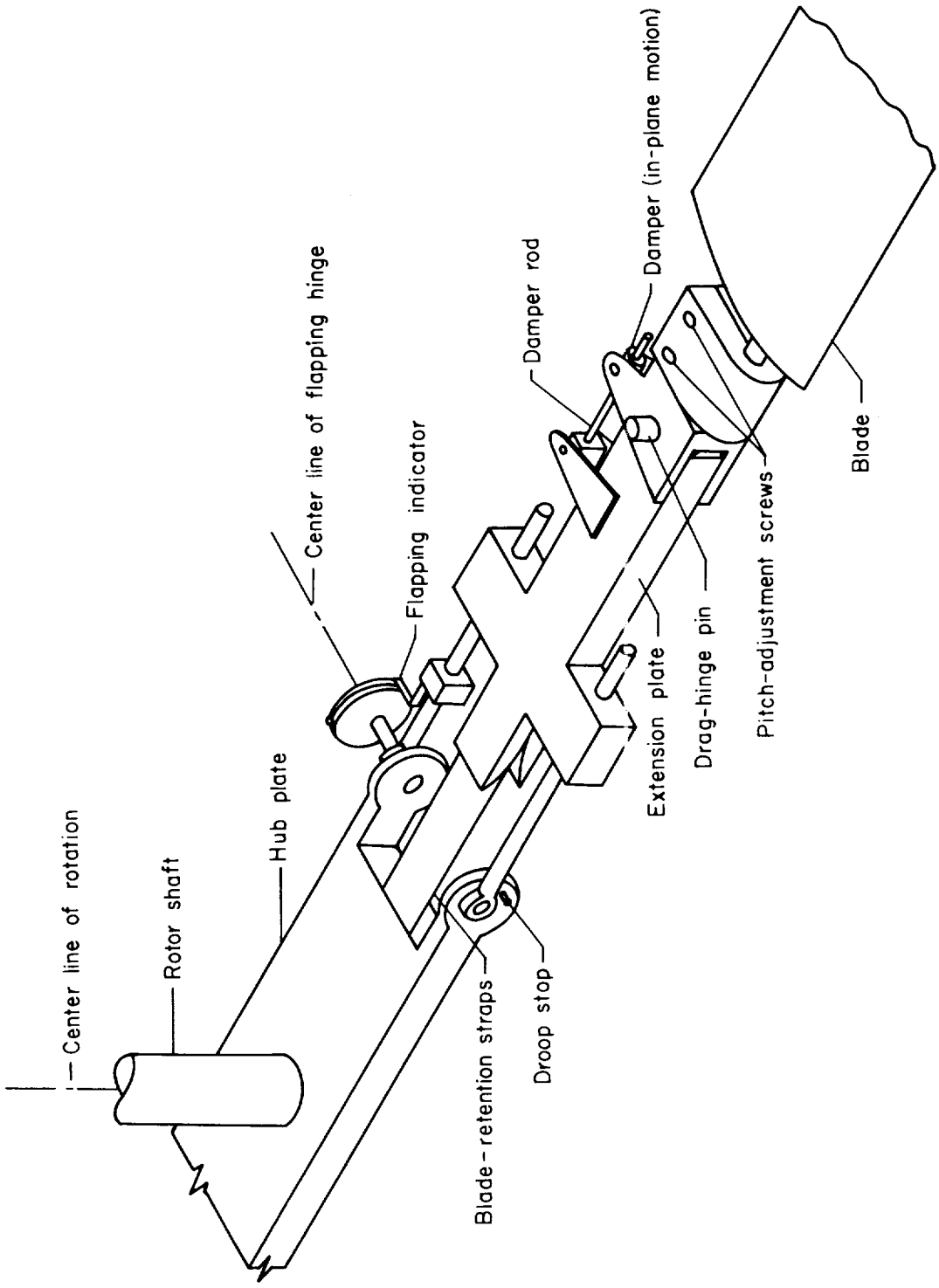

Figure 2.- Blade root fitting for flapping-hinge-offset configuration.

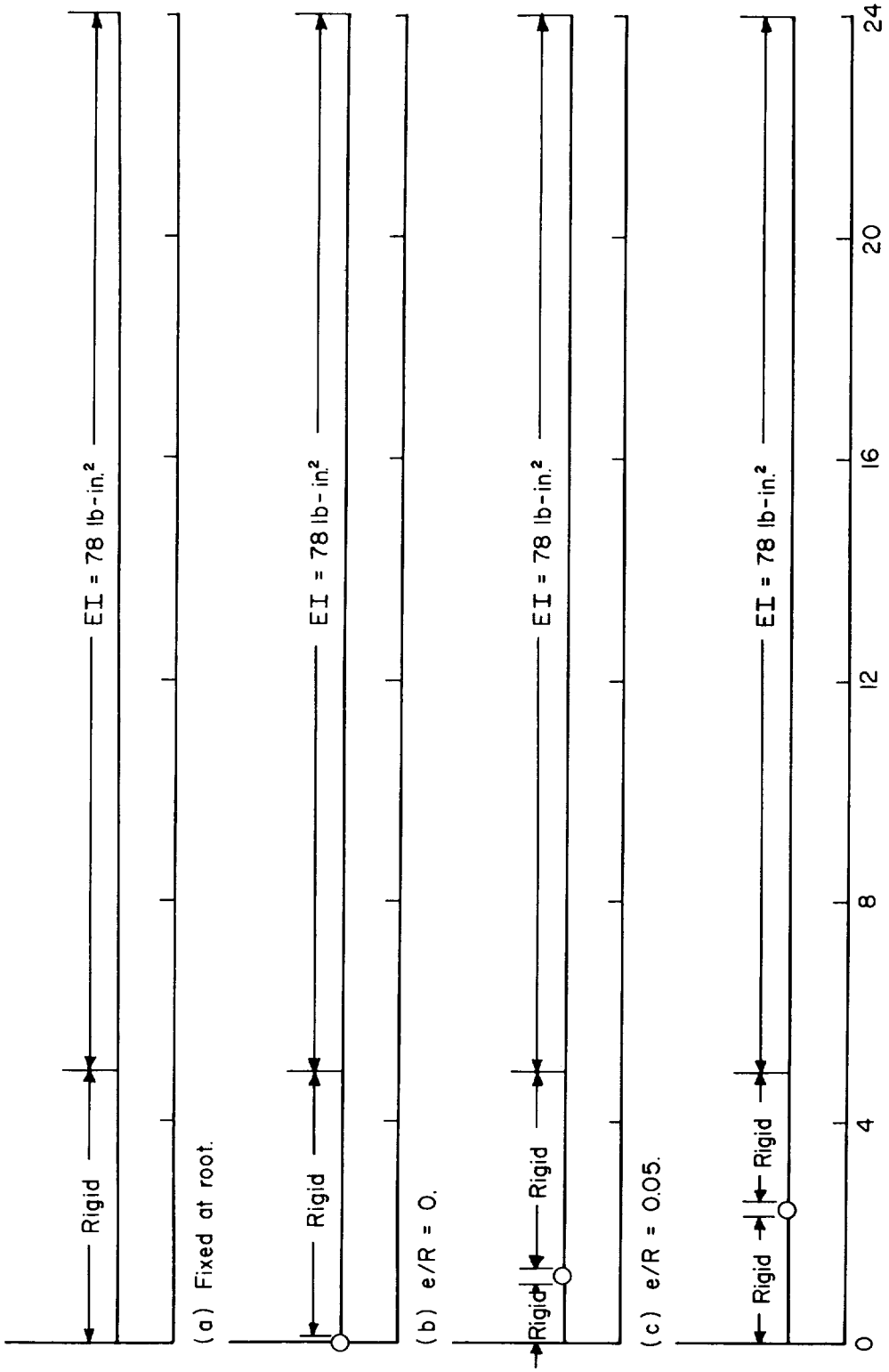

Figure 3.- Blade spanwise stiffness distribution for the different root configurations.

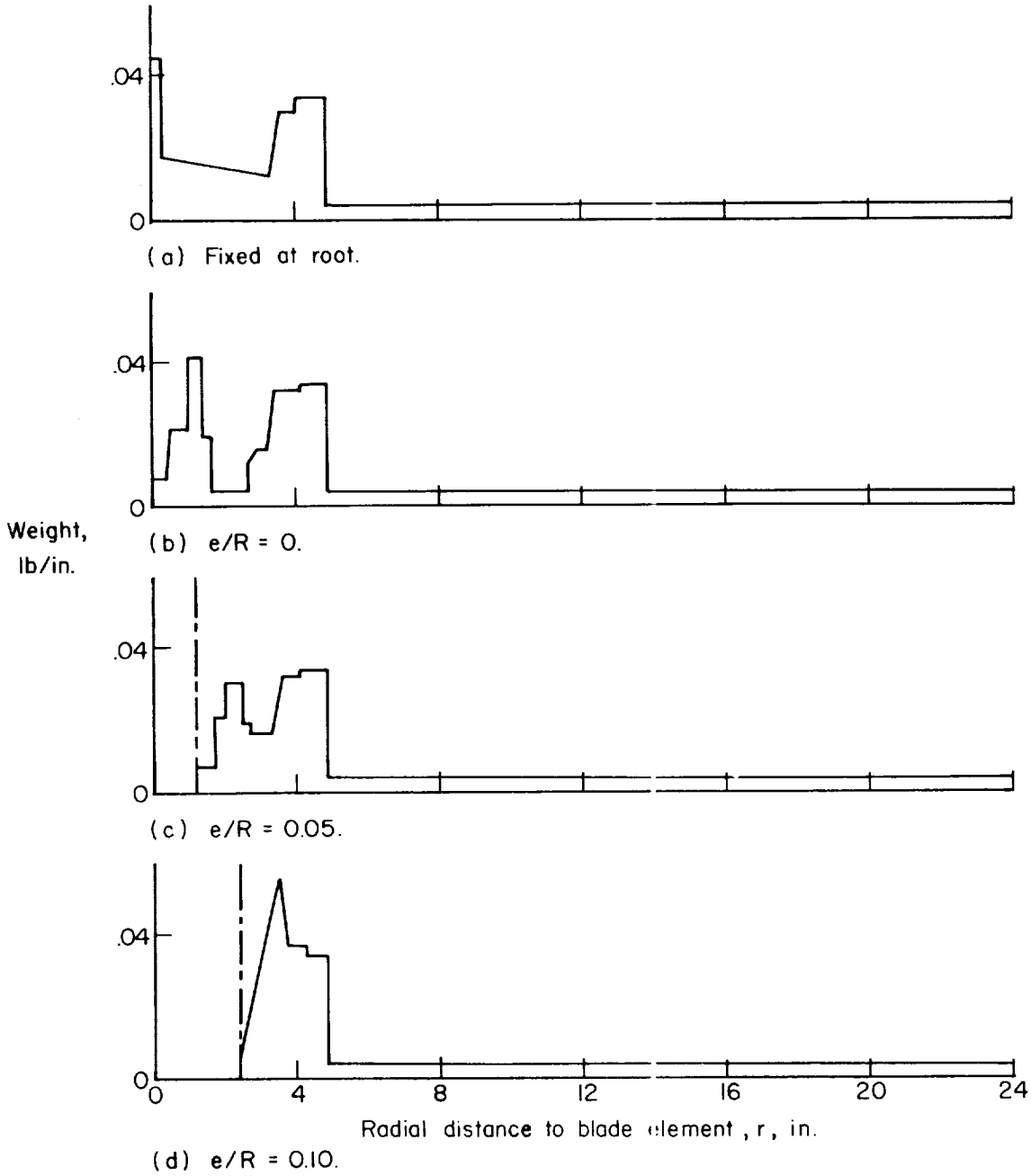

Figure 4.- Blade spanwise weight distributions for the different root configurations.

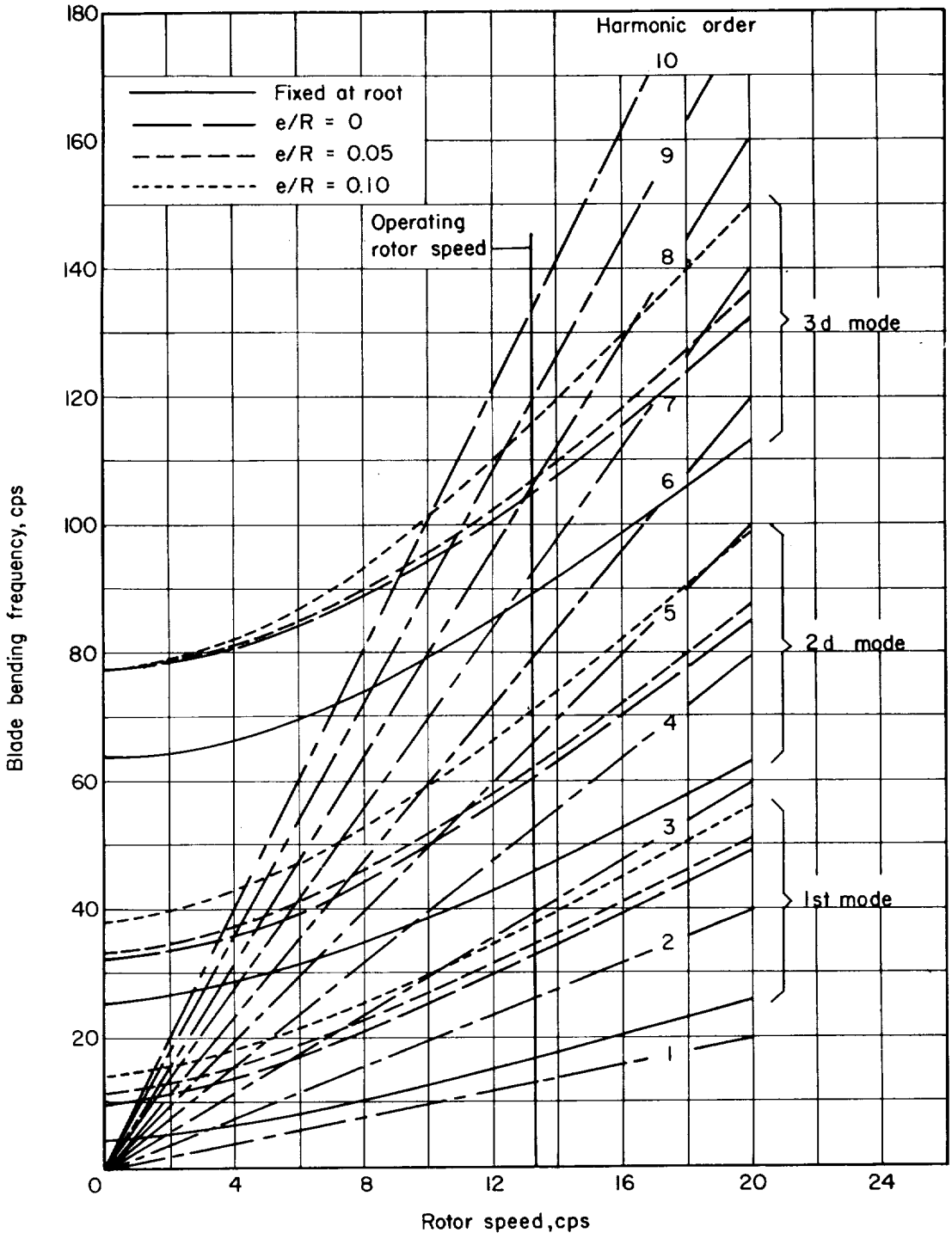

Figure 5.- Variation of blade bending frequency with rotor speed for first three modes for various root fittings.

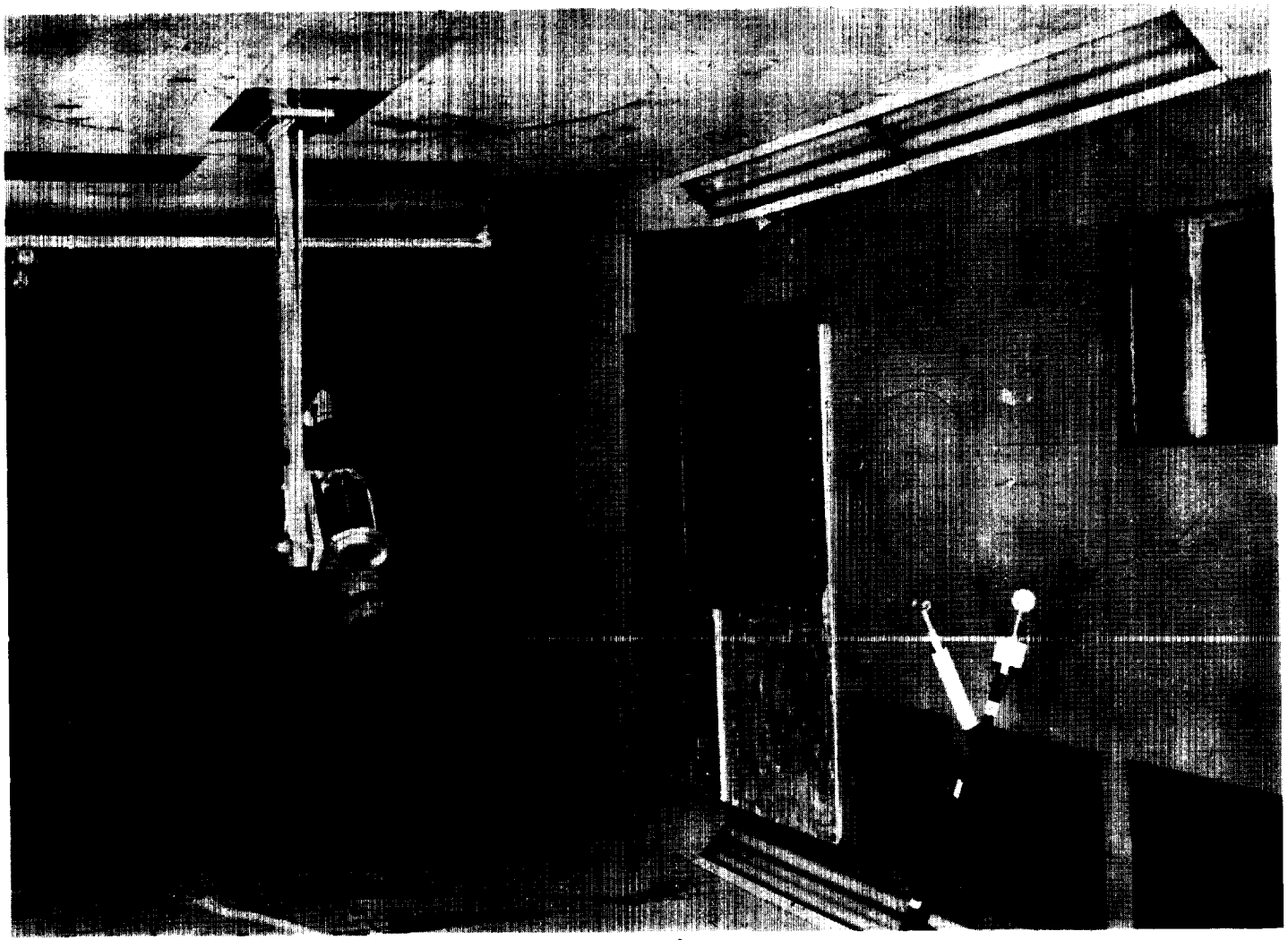

L-58-88

Figure 6.- Model mounted in tunnel test section. ($\alpha = 40^{\circ}$, looking downstream.)

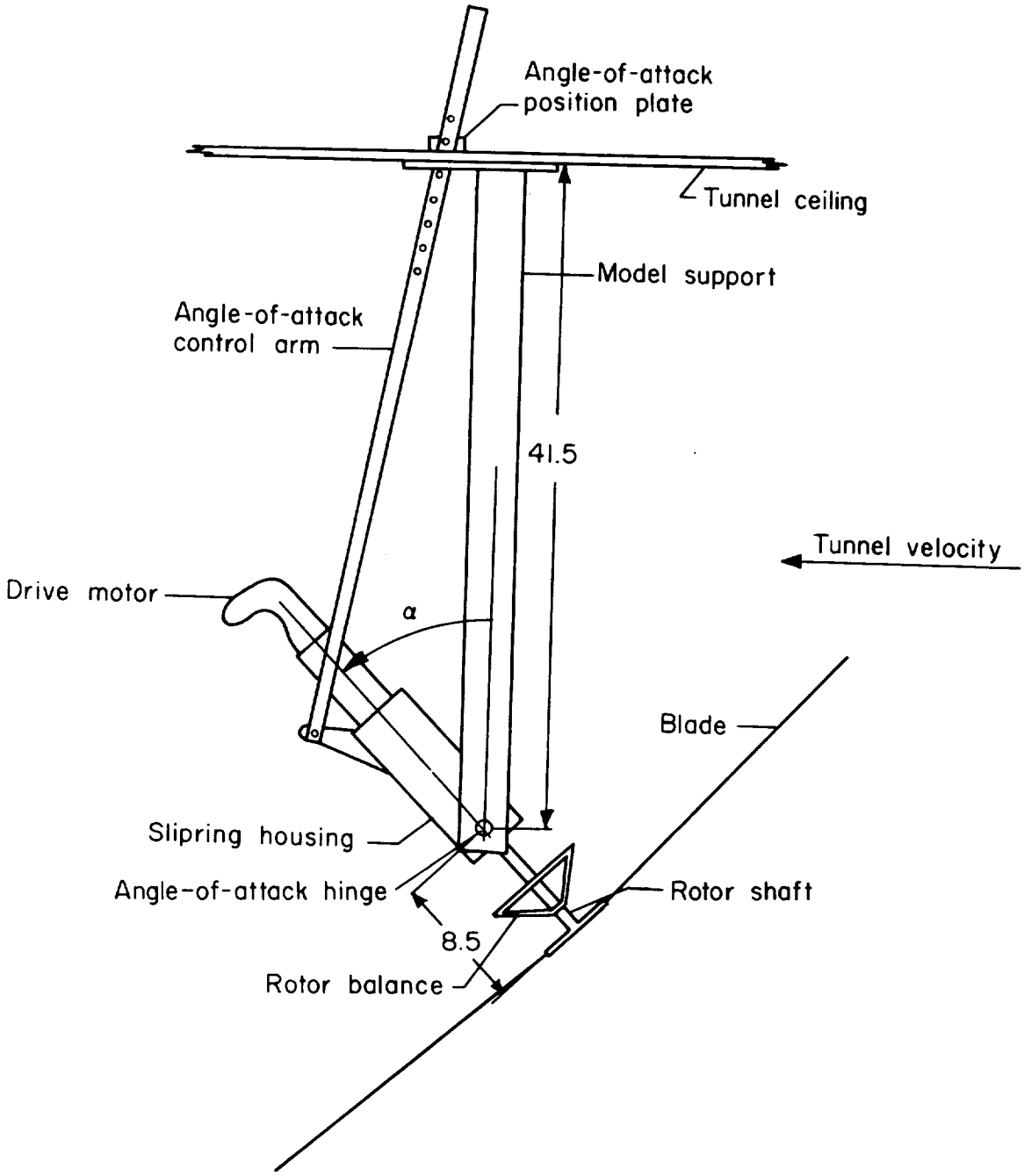

Figure 7.- Model support showing method of varying rotor angle of attack. Dimensions are in inches.

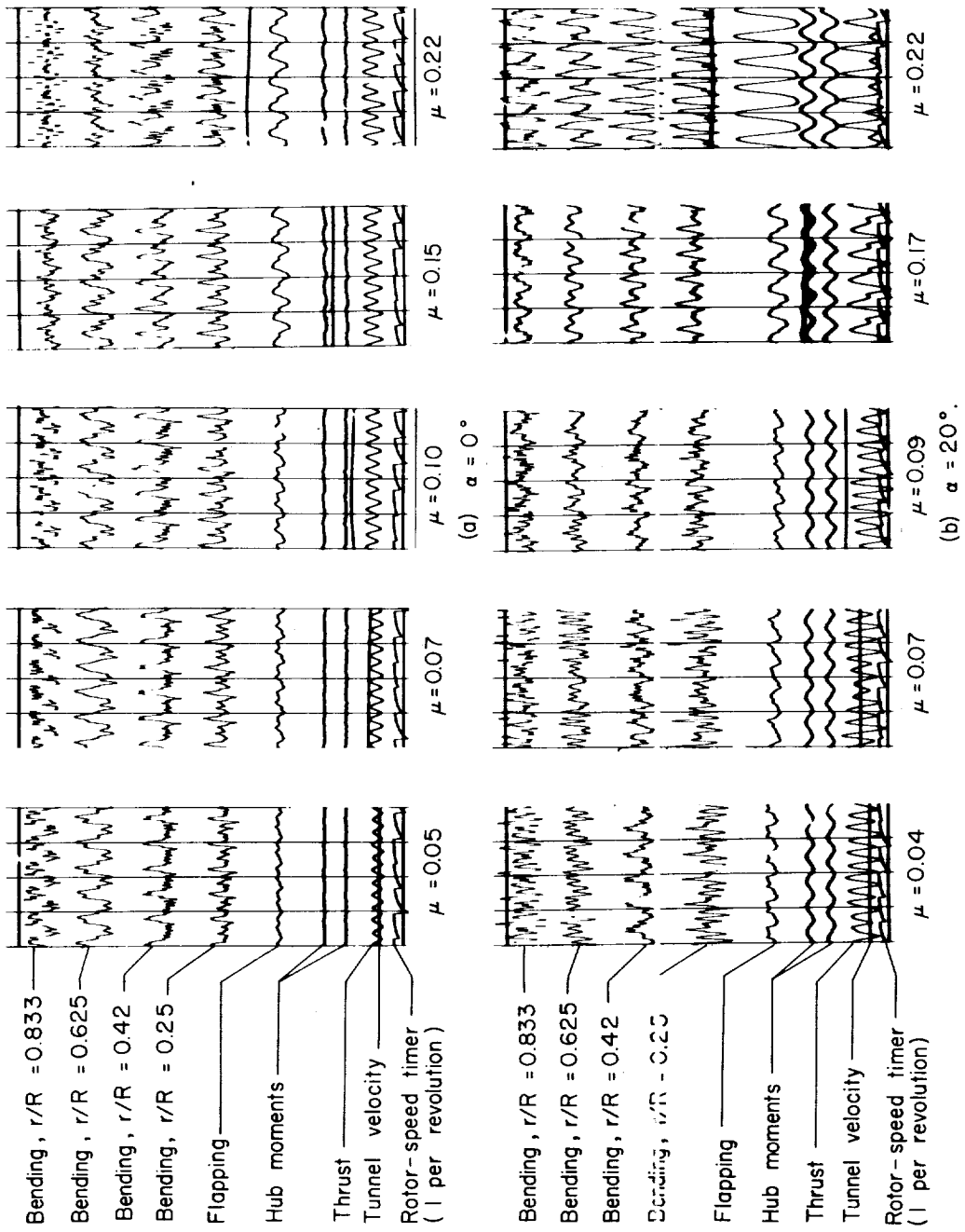

Figure 8.- Sections of typical records showing effect of tip-speed ratio on frequency content. e/R = 0; θ = 3°.

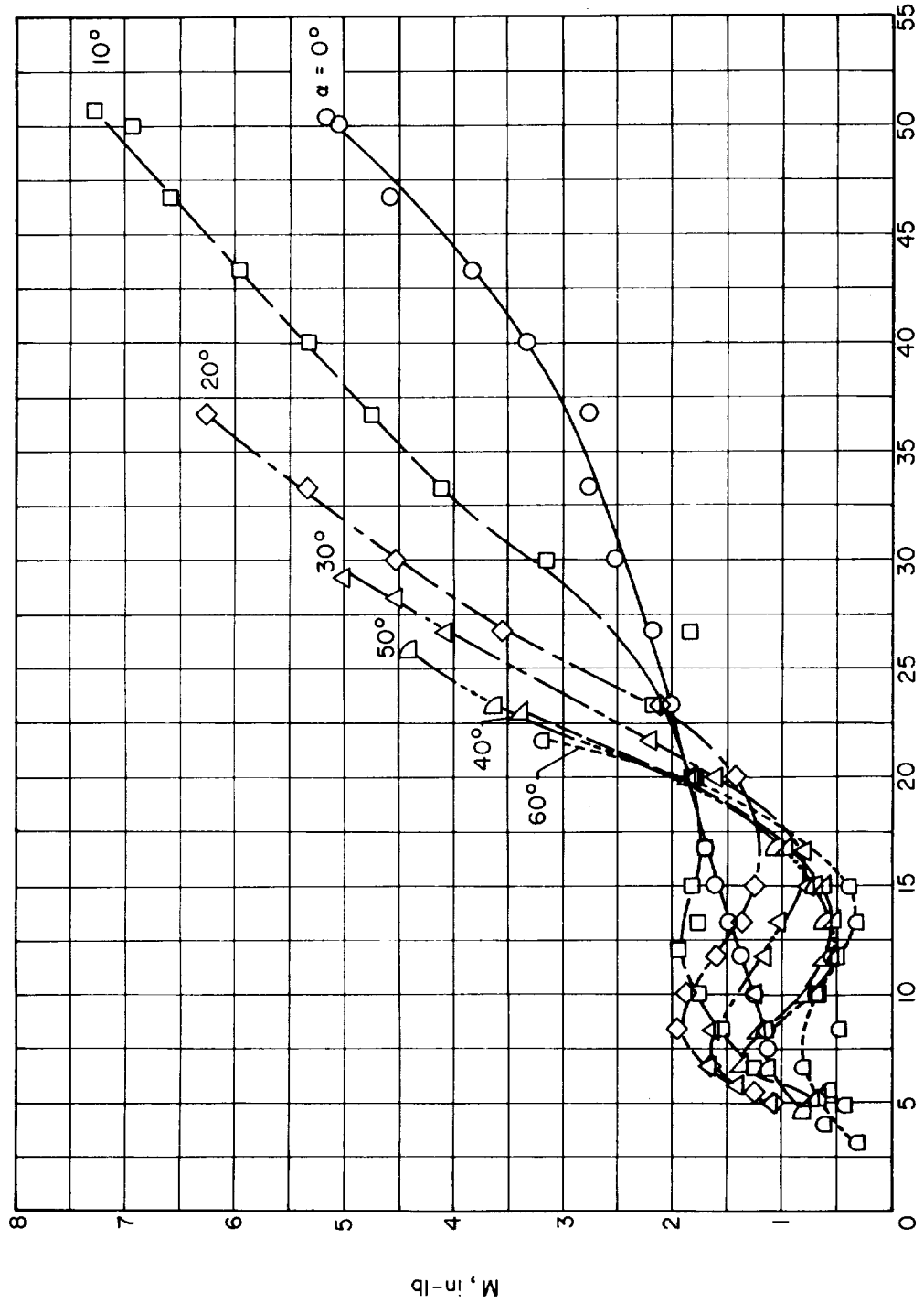

Figure 9.- Typical variation of double-amplitude blade periodic bending moment with tunnel velocity.

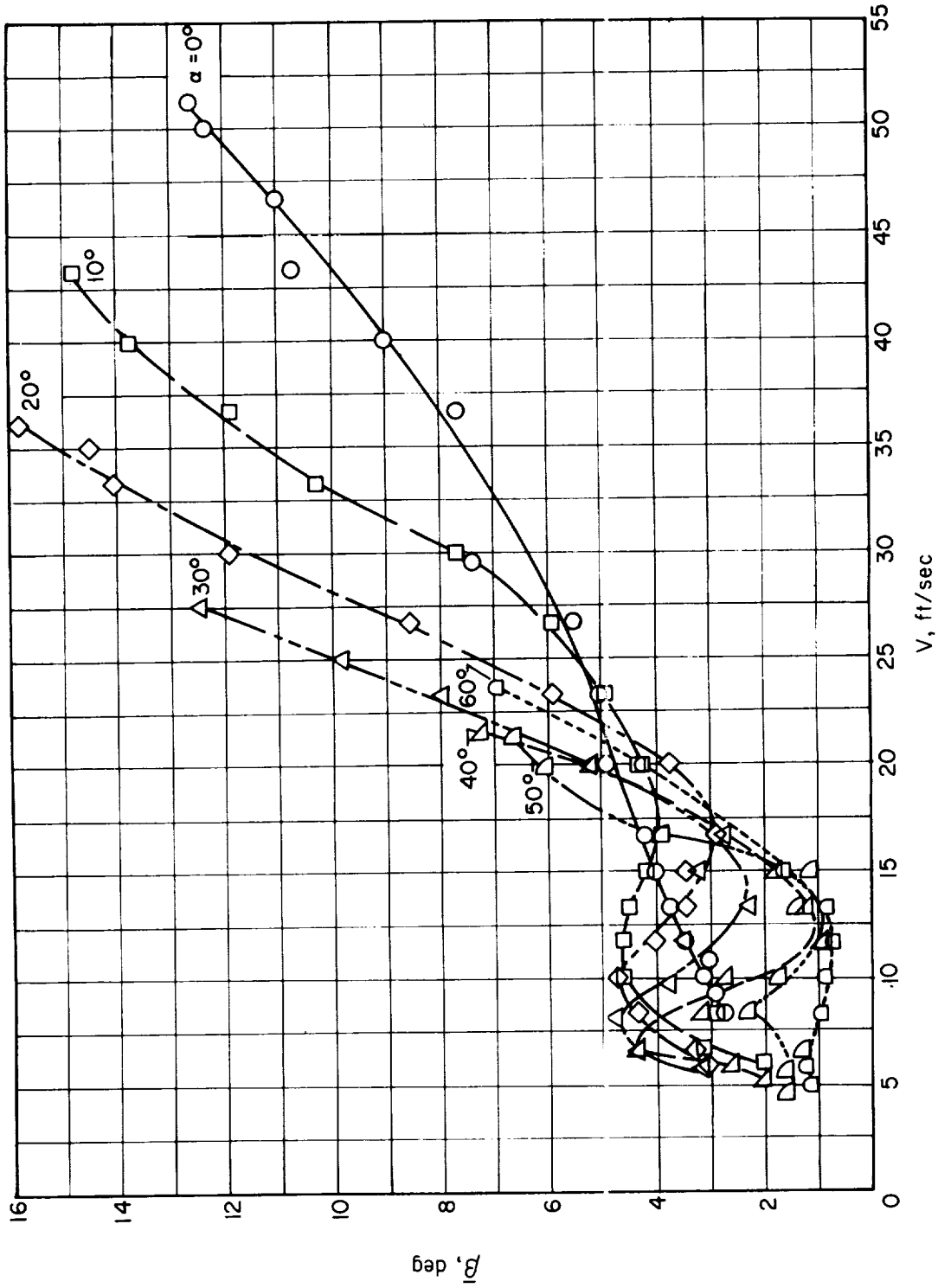

Figure 10.- Typical variation of double-amplitude blade periodic flapping with tunnel velocity.

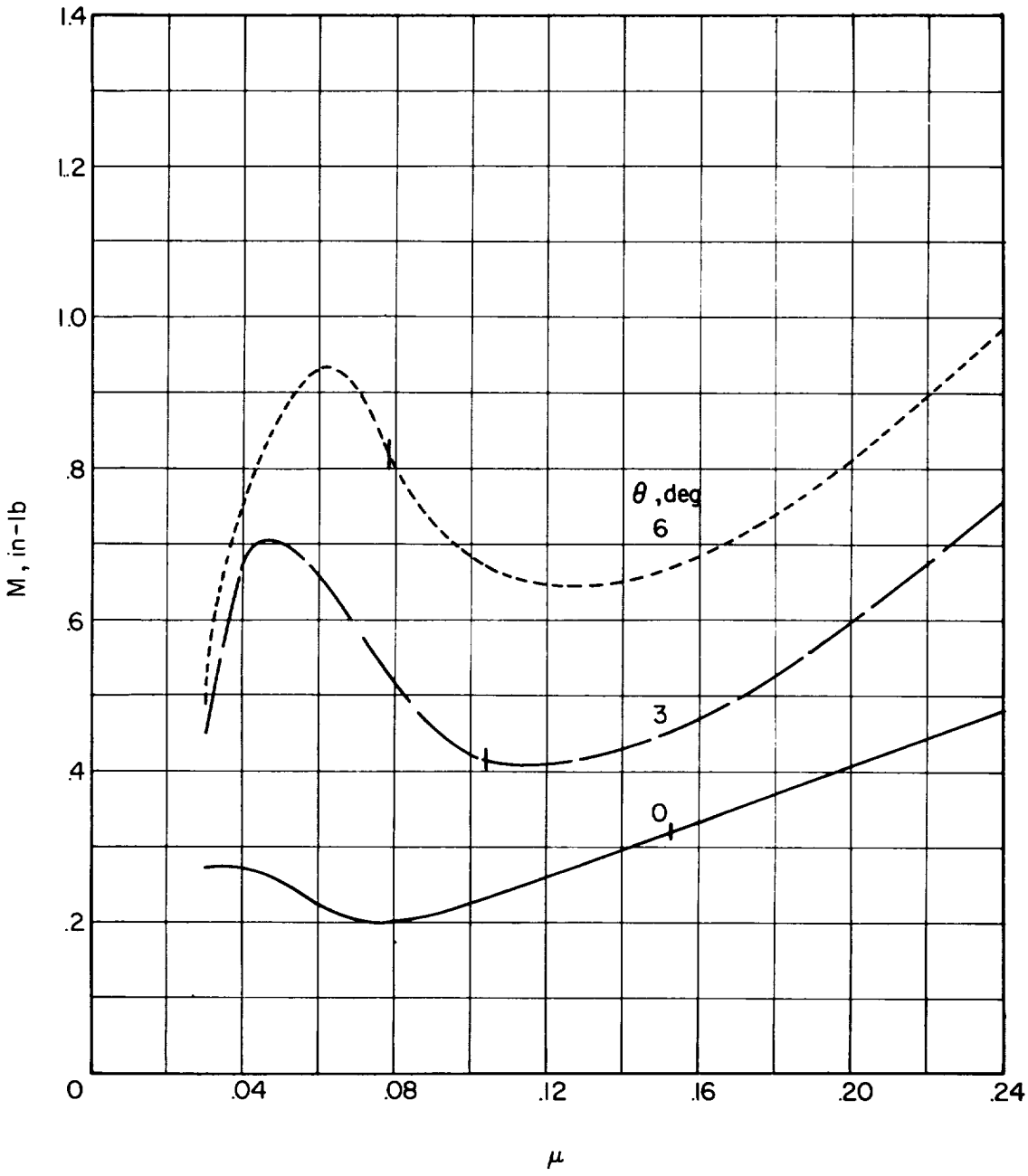

Figure 11.- Effect of collective pitch angle on double-amplitude blade periodic bending moment as a function of tip-speed ratio. $e/R = 0$; $\alpha = 20^{\circ}$; $r/R = 0.25$. (Short vertical lines indicate values of μ at which stall effects are assumed to be significant.)

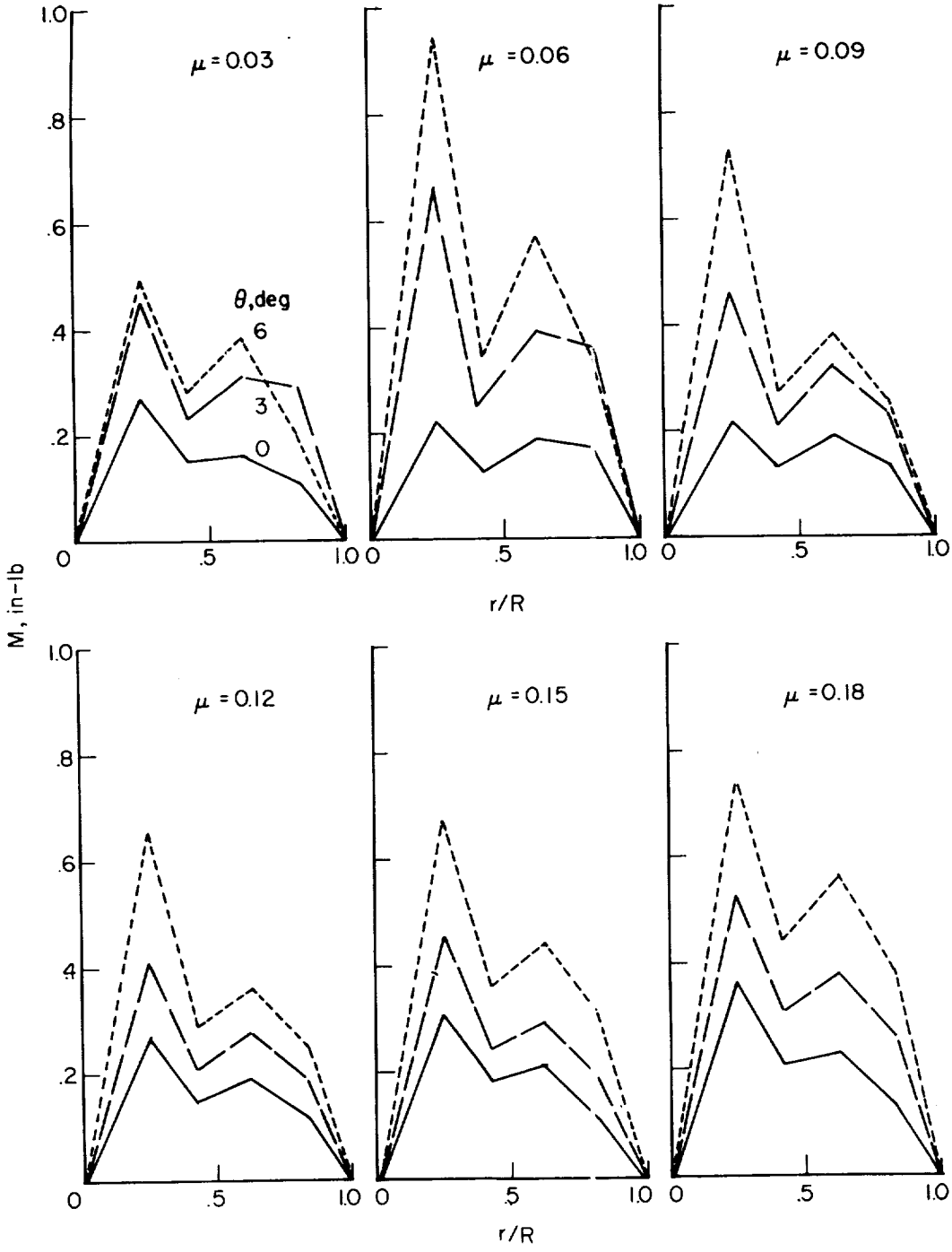

Figure 12.- Effect of collective pitch angle on double-amplitude blade periodic bending moment as a function of fraction of blade radius. e/R = 0; $\alpha = 20^{\circ}$.

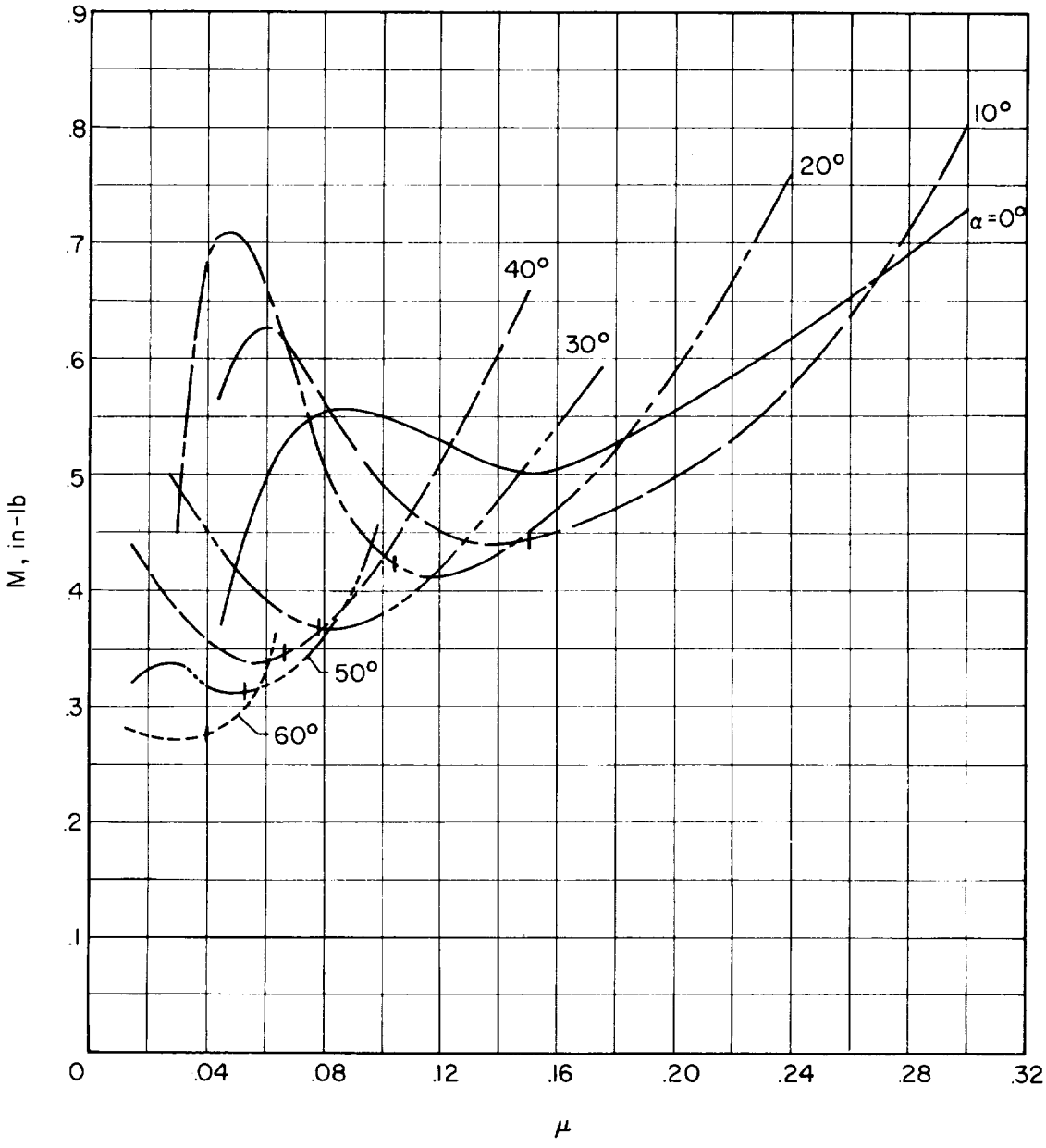

Figure 13.- Effect of rotor angle of attack on double-amplitude blade periodic bending moment as a function of tip-speed ratio. $e/R = 0$; $r/R = 0.25$; $\theta = 3^{\circ}$. (Short vertical lines indicate values of μ at which stall effects are assumed to be significant.)

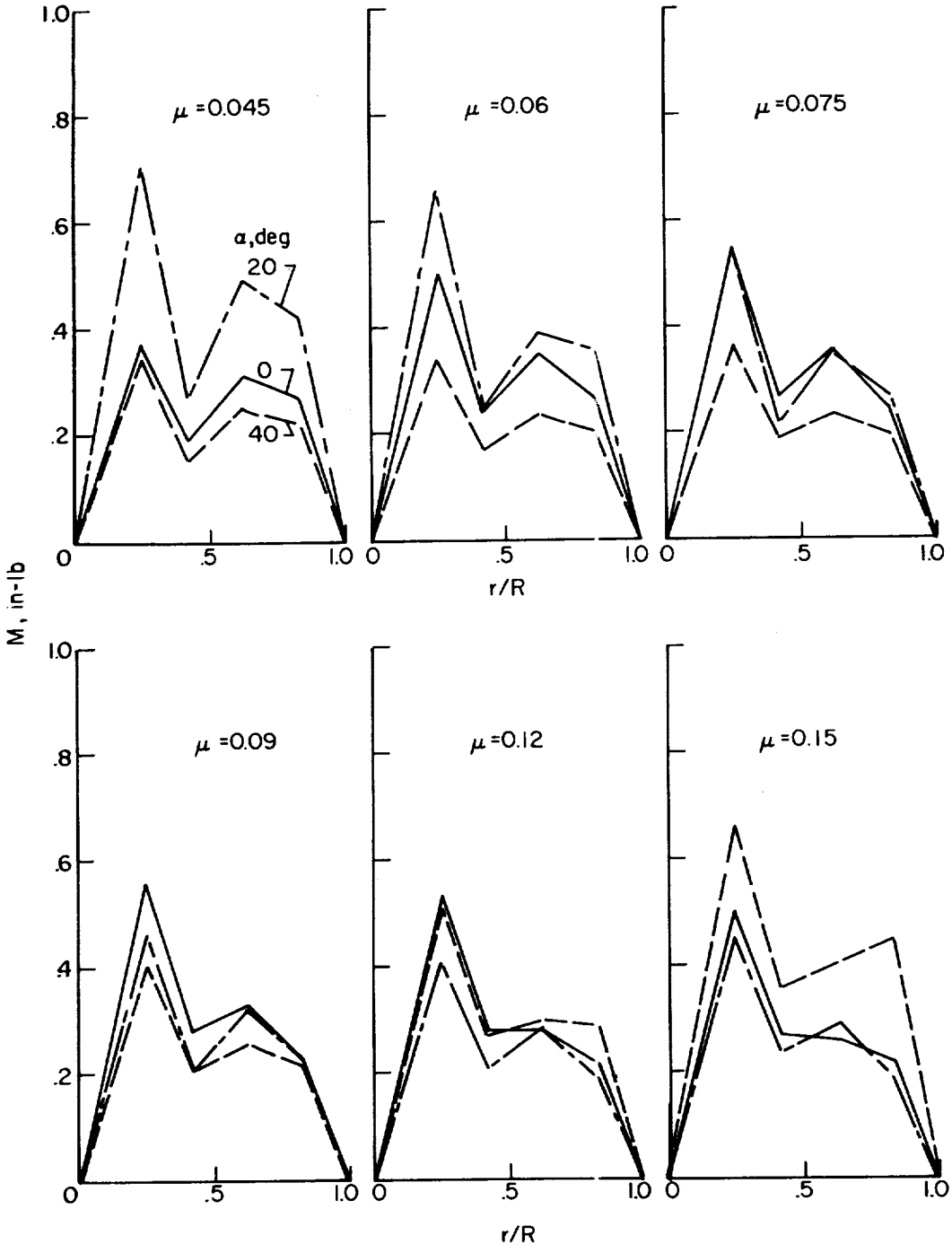

Figure 14.- Effect of rotor angle of attack on double-amplitude blade periodic bending moment as a function of fraction of blade radius. $e/R = 0$; $\theta = 3^{\circ}$.

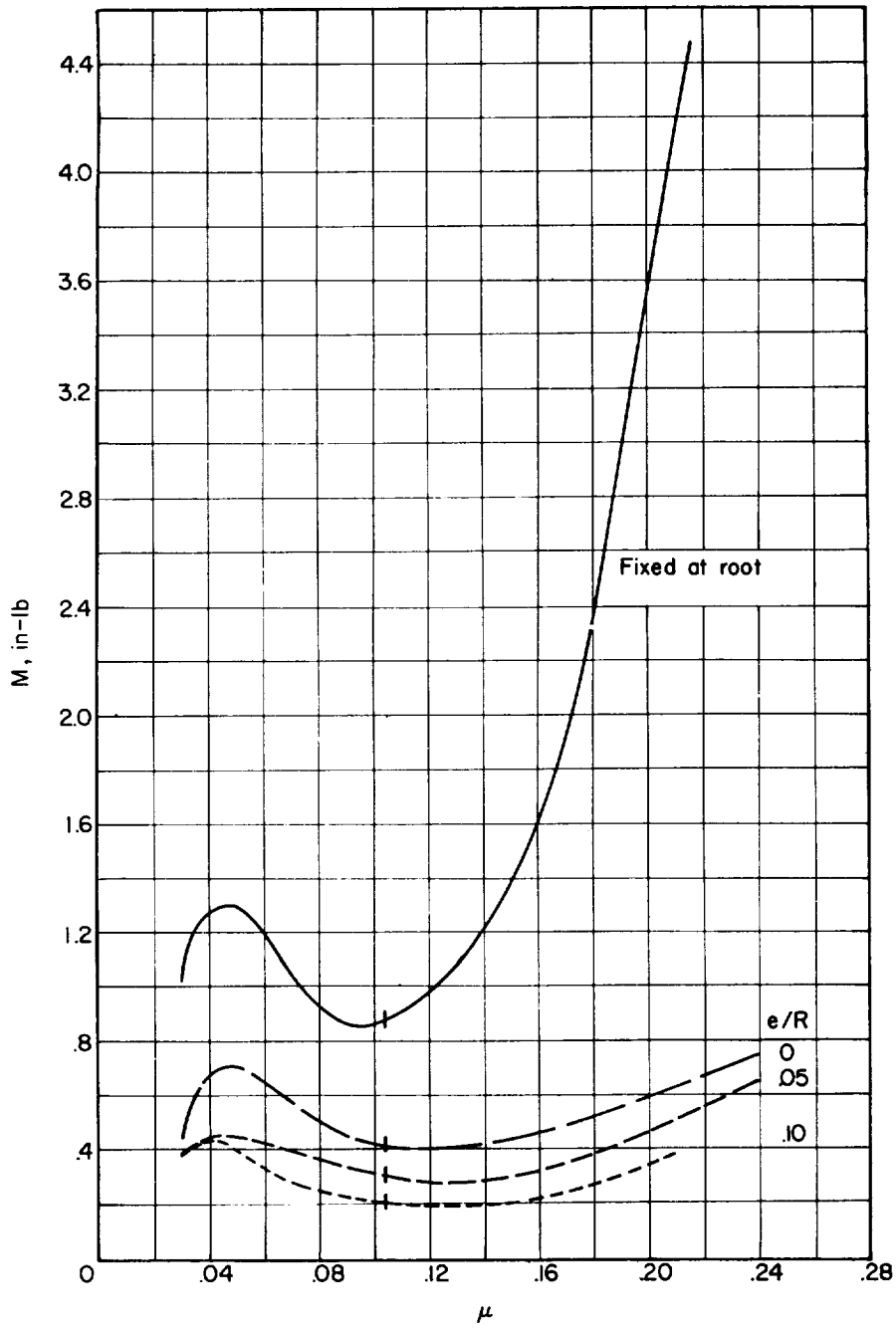

Figure 15.- Effect of flapping-hinge offset on double-amplitude blade periodic bending moment as a function of tip-speed ratio. $\alpha = 20^{\circ}$; $\theta = 3^{\circ}$; $r/R = 0.25$. (Short vertical lines indicate values of μ at which stall effects are assumed to be significant.)

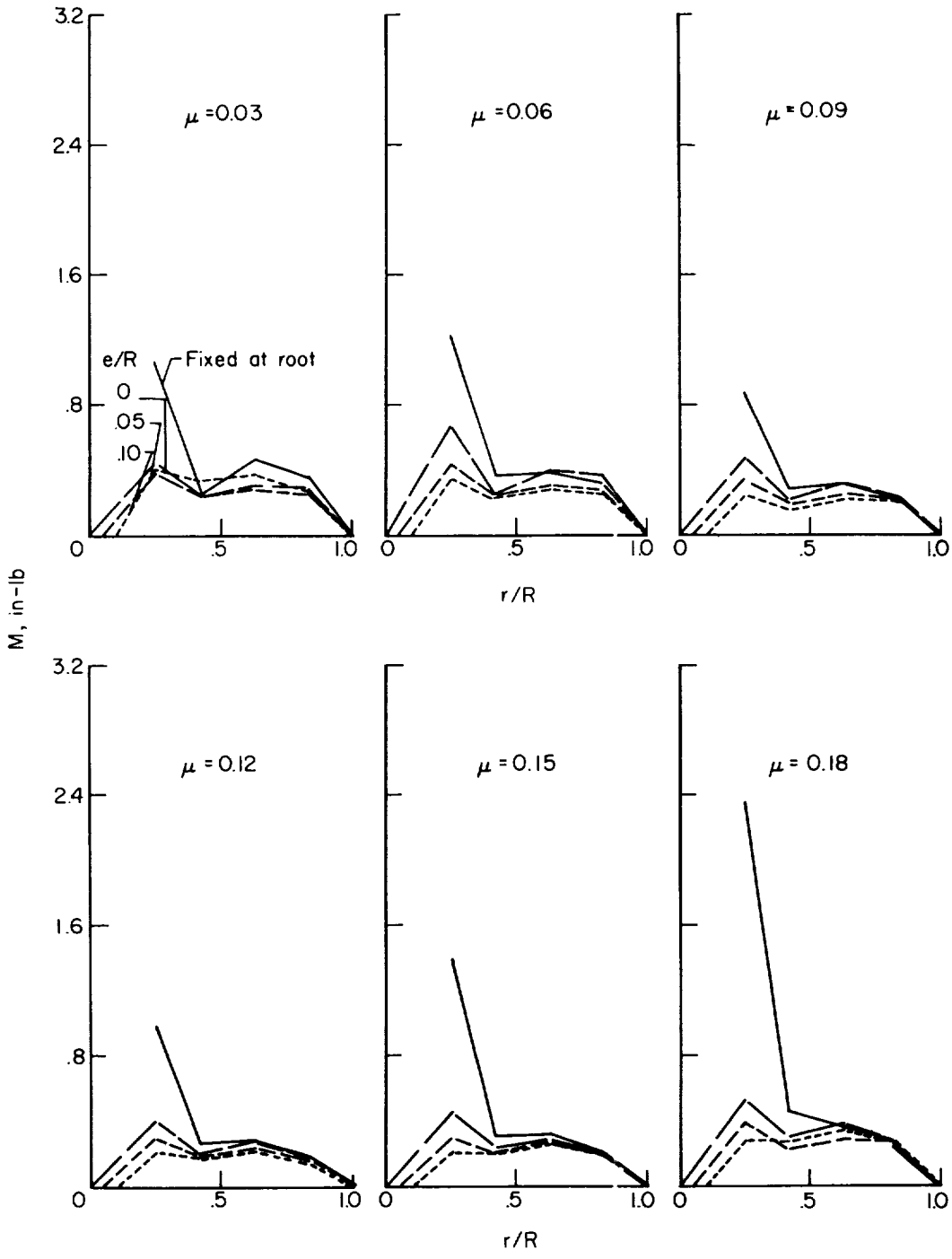

Figure 16.- Effect of flapping-hinge offset on double-amplitude blade periodic bending moment as a function of fraction of blade radius. $\alpha = 20^{\circ}$; $\theta = 3^{\circ}$.

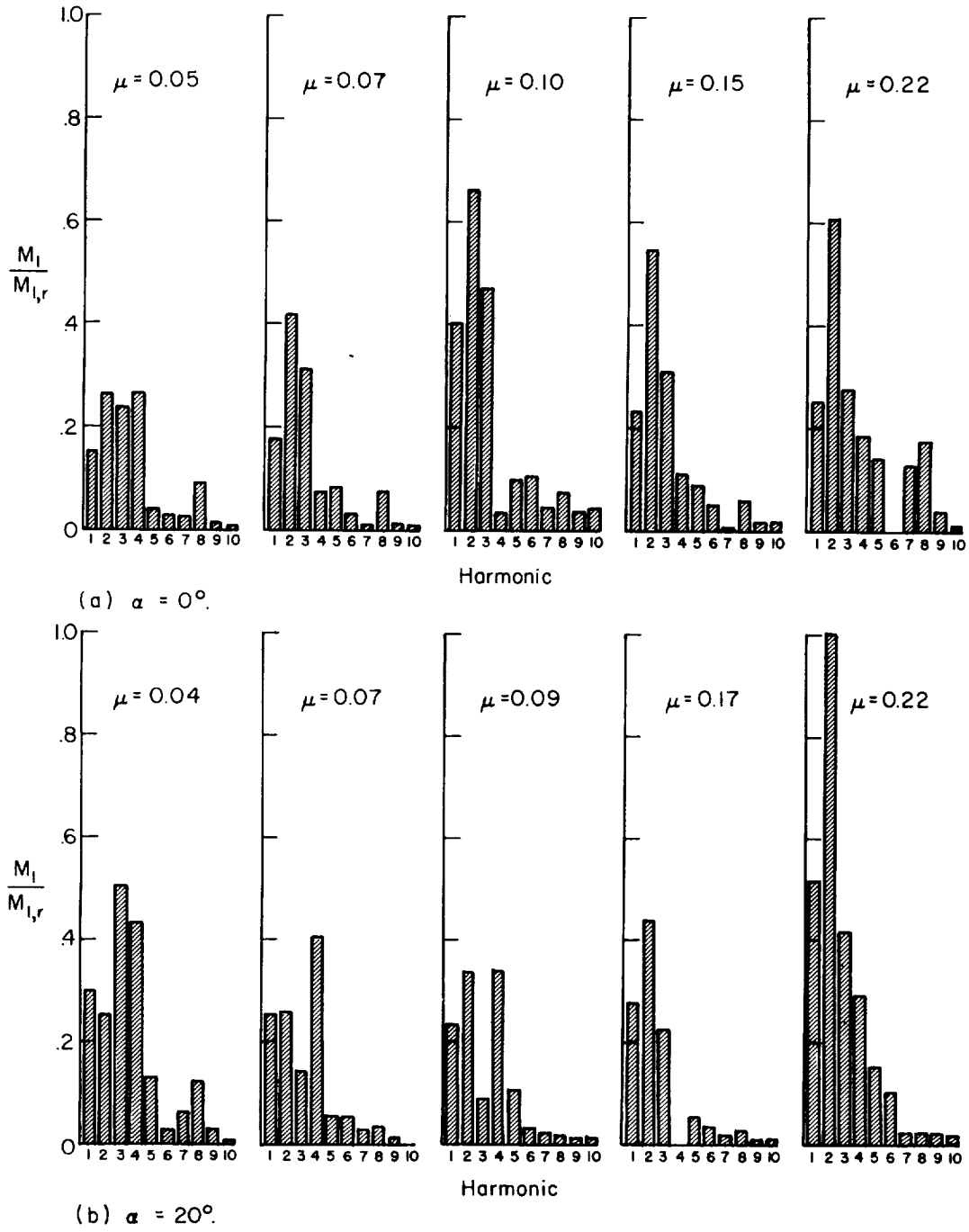

Figure 17.- Harmonic content of double-amplitude blade periodic bending moment at station $r/R = 0.25$ as a function of tip-speed ratio. $e/R = 0$; $\theta = 3°$; $M_{l,r} = 0.47$ in-lb, double amplitude.

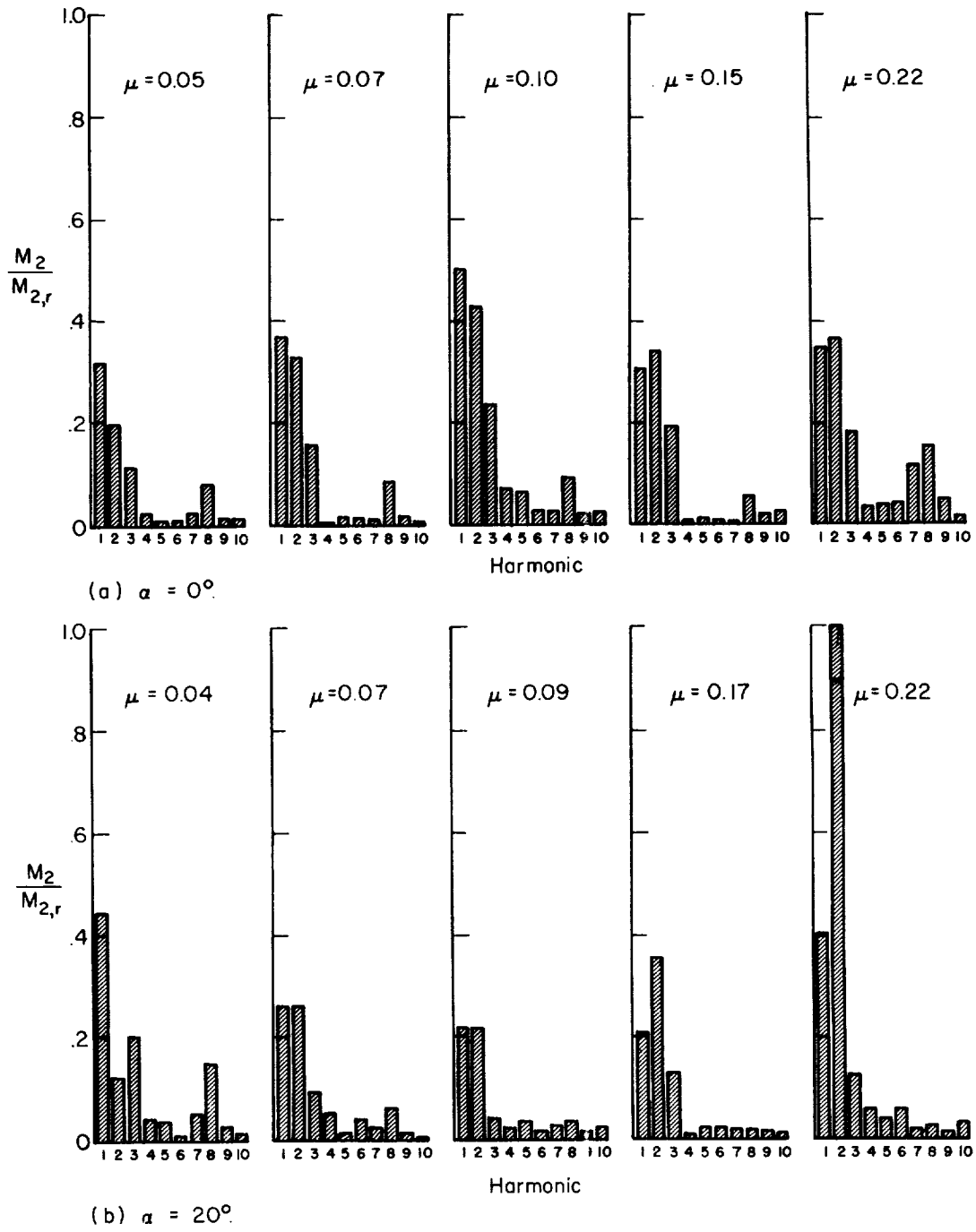

Figure 18.- Harmonic content of double-amplitude blade periodic bending moment at station r/R = 0.42 as a function of tip-speed ratio. e/R = 0; θ = 3°; $M_{2,r}$ = 0.33 in-lb, double amplitude.

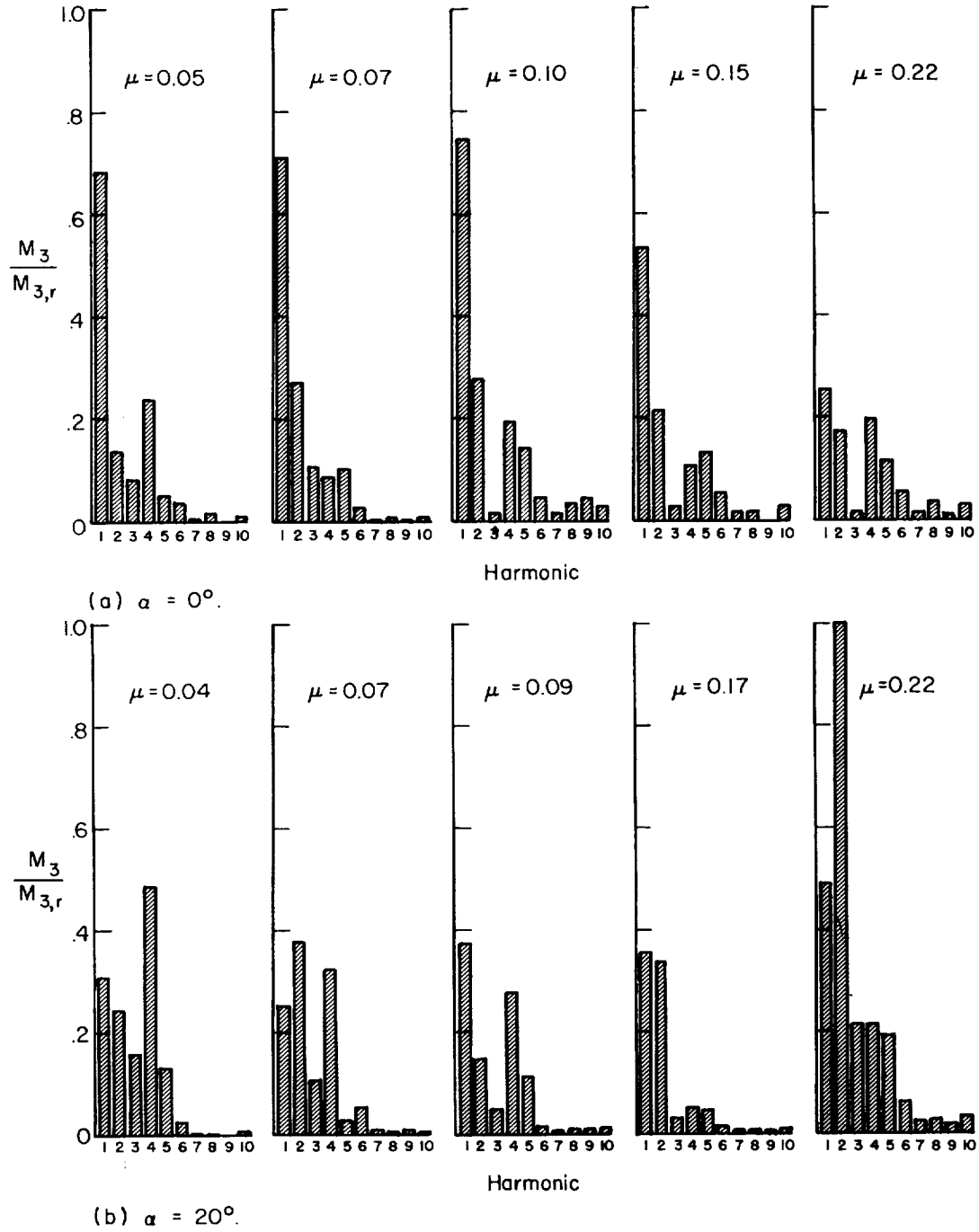

Figure 19.- Harmonic content of double-amplitude blade periodic bending moment at station $r/R = 0.625$ as a function of tip-speed ratio. $e/R = 0$; $\theta = 3°$; $M_{3,r} = 0.36$ in-lb, double amplitude.

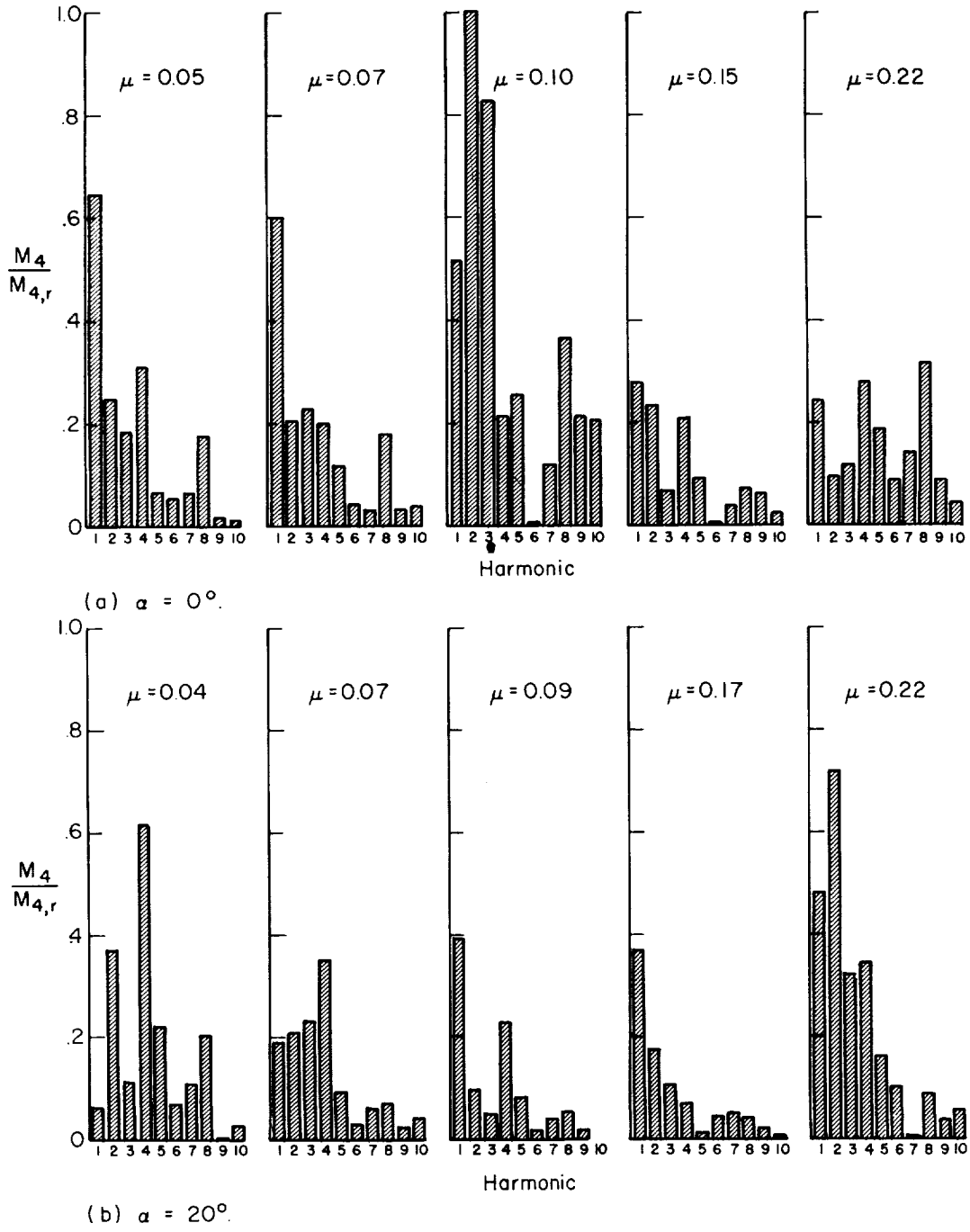

Figure 20.- Harmonic content of double-amplitude blade periodic bending moment at station $r/R = 0.833$ as a function of tip-speed ratio. $e/R = 0$; $\theta = 3^{\circ}$; $M_{4,r} = 0.28$ in-lb, double amplitude.

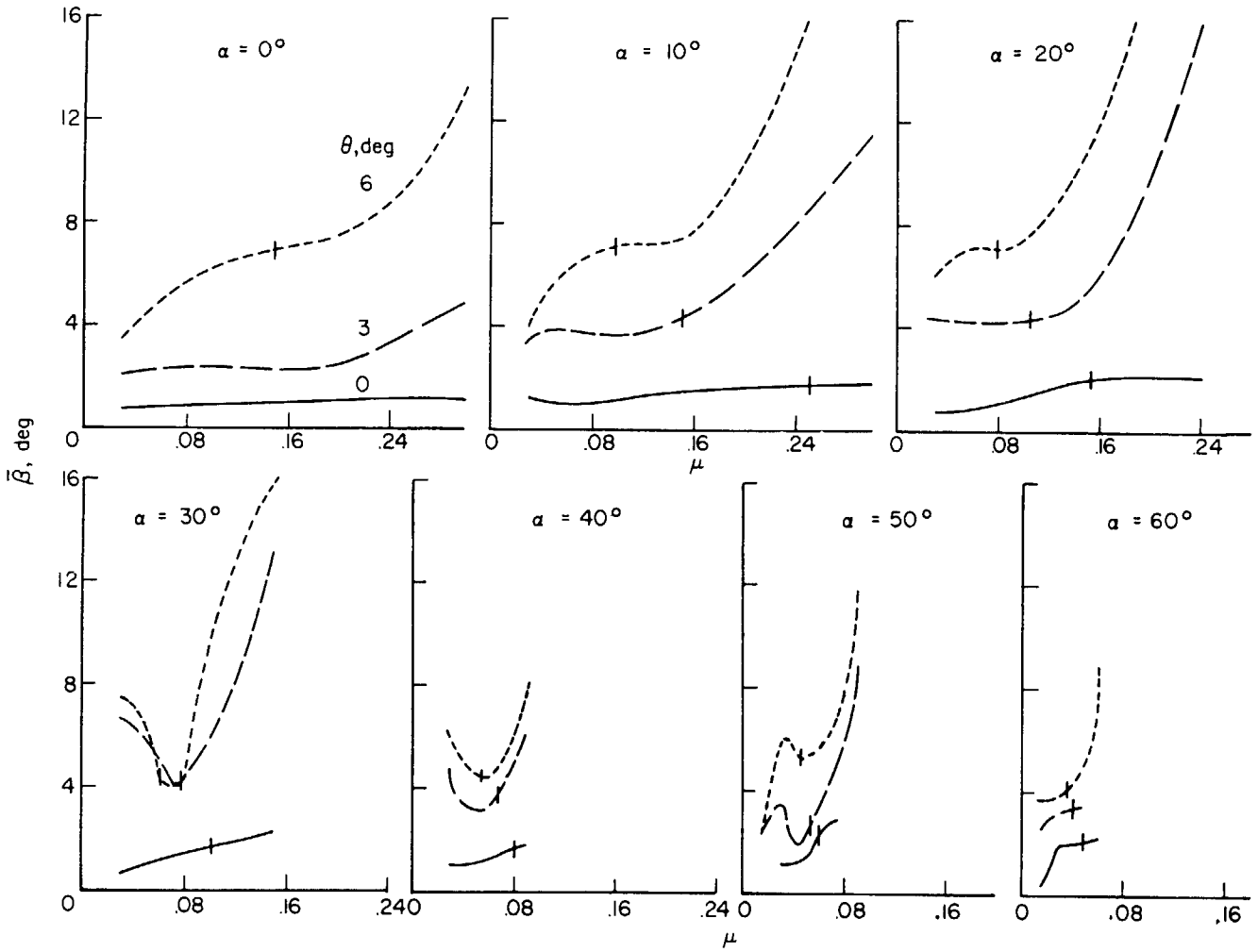

Figure 21.- Effect of collective pitch angle on double-amplitude blade periodic flapping as a function of tip-speed ratio. e/R = 0.05. (Short vertical lines indicate values of μ at which stall effects are assumed to be significant.)

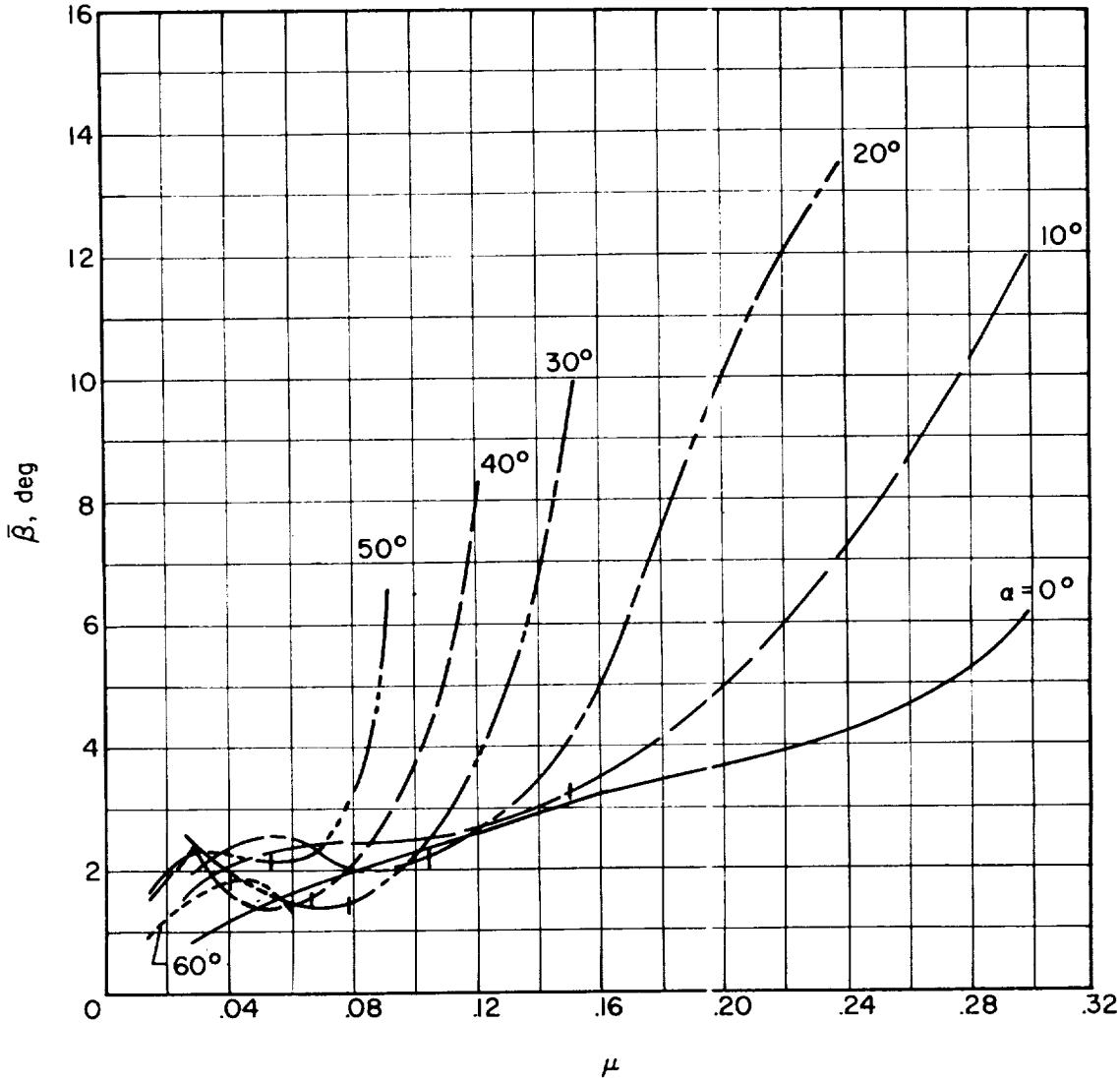

Figure 22.- Effect of rotor angle of attack on double-amplitude blade periodic flapping as a function of tip-speed ratio. $e/R = 0$; $\theta = 3^\circ$. (Short vertical lines indicate values of μ at which stall effects are assumed to be significant.)

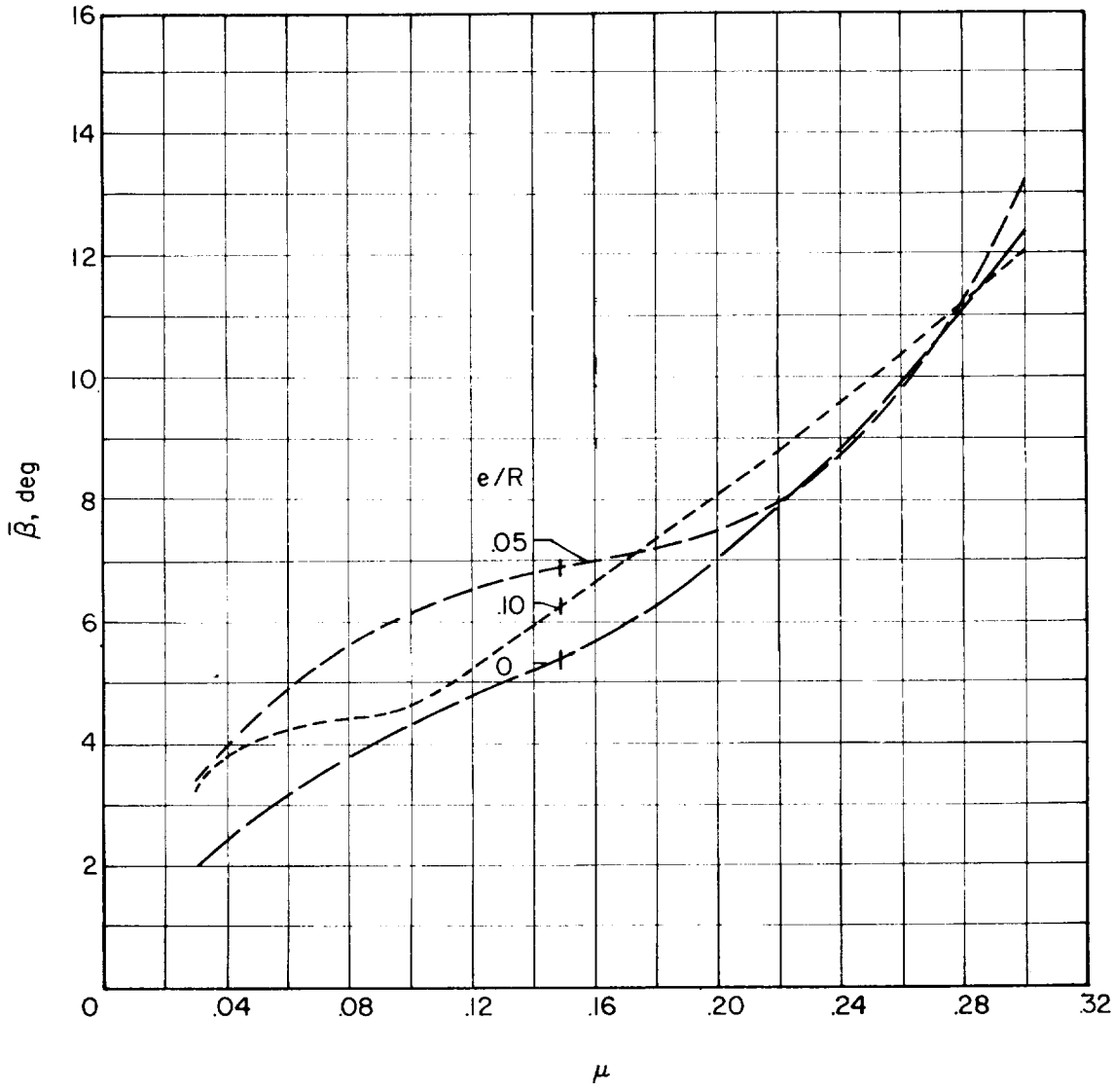

Figure 23.- Effect of flapping-hinge offset on double-amplitude blade periodic flapping as a function of tip-speed ratio. $\alpha = 0^\circ$; $\theta = 6^\circ$. (Short vertical lines indicate values of μ at which stall effects are assumed to be significant.)

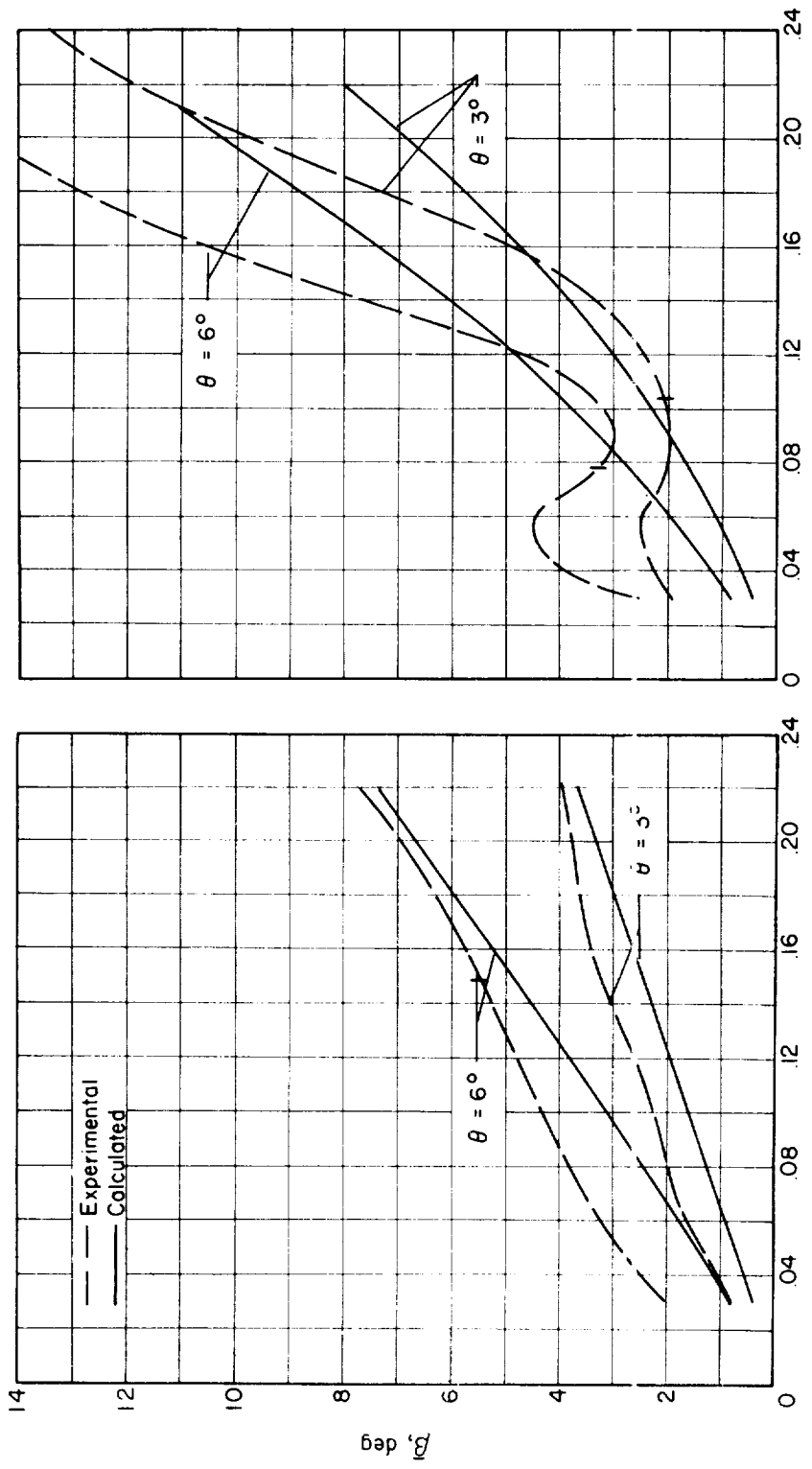

Figure 24.- Comparison of experimental and calculated double-amplitude blade periodic flapping angles. $e/R = 0$. (Short vertical lines indicate values of μ at which stall effects are assumed to be significant.)